

# Nanoparticulate STING agonists are potent lymph node–targeted vaccine adjuvants

Melissa C. Hanson,<sup>1,2</sup> Monica P. Crespo,<sup>2</sup> Wuhbet Abraham,<sup>2</sup> Kelly D. Moynihan,<sup>1,2,3</sup> Gregory L. Szeto,<sup>1,2,3,4</sup> Stephanie H. Chen,<sup>4</sup> Mariane B. Melo,<sup>2</sup> Stefanie Mueller,<sup>2</sup> and Darrell J. Irvine<sup>1,2,3,4,5</sup>

<sup>1</sup>Department of Biological Engineering and <sup>2</sup>David H. Koch Institute for Integrative Cancer Research, Massachusetts Institute of Technology, Cambridge, Massachusetts, USA. <sup>3</sup>The Ragon Institute of MGH, MIT, and Harvard, Cambridge, Massachusetts, USA. <sup>4</sup>Department of Materials Science and Engineering, Massachusetts Institute of Technology, Cambridge, Massachusetts, USA.

<sup>5</sup>Howard Hughes Medical Institute, Chevy Chase, Maryland, USA.

Cyclic dinucleotides (CDNs) are agonists of stimulator of IFN genes (STING) and have potential as vaccine adjuvants. However, cyclic di-GMP (cdGMP) injected s.c. shows minimal uptake into lymphatics/draining lymph nodes (dLNs) and instead is rapidly distributed to the bloodstream, leading to systemic inflammation. Here, we encapsulated cdGMP within PEGylated lipid nanoparticles (NP-cdGMP) to redirect this adjuvant to dLNs. Compared with unformulated CDNs, encapsulation blocked systemic dissemination and markedly enhanced dLN accumulation in murine models. Delivery of NP-cdGMP increased CD8<sup>+</sup> T cell responses primed by peptide vaccines and enhanced therapeutic antitumor immunity. A combination of a poorly immunogenic liposomal HIV gp41 peptide antigen and NP-cdGMP robustly induced type I IFN in dLNs, induced a greater expansion of vaccine-specific CD4<sup>+</sup> T cells, and greatly increased germinal center B cell differentiation in dLNs compared with a combination of liposomal HIV gp41 and soluble CDN. Further, NP-cdGMP promoted durable antibody titers that were substantially higher than those promoted by the well-studied TLR agonist monophosphoryl lipid A and comparable to a much larger dose of unformulated cdGMP, without the systemic toxicity of the latter. These results demonstrate that nanoparticulate delivery safely targets CDNs to the dLNs and enhances the efficacy of this adjuvant. Moreover, this approach can be broadly applied to other small-molecule immunomodulators of interest for vaccines and immunotherapy.

## Introduction

The development of structure-based vaccinology using well-defined subunit antigens has enabled the development of vaccines with excellent safety profiles, but this increase in safety has been accompanied by a decrease in immunogenicity compared with traditional live-attenuated vaccines. Thus, adjuvants have become essential components of vaccine formulations in order to promote durable and effective immune responses to subunit vaccines (1–3). Traditional adjuvants, such as aluminum salts and water/oil emulsions, have set the standard for safety and efficacy in vaccine development but fail to elicit effective immune responses to many candidate antigens, and diverse new adjuvant formulations have been pursued in both academic and industrial vaccine research (4). Advances in our understanding of innate immunity have enabled the identification of new danger-sensing receptors relevant for the design of molecular adjuvants acting on defined innate immune signaling pathways. In particular, pattern recognition receptors (PRRs) are key sensors of the innate immune system whose role is to identify pathogenic microorganisms and promote appropriate immune responses. The most-studied PRRs so far are the TLRs, and monophosphoryl lipid A (MPLA), a derivative of lipopolysaccharide that binds TLR4, is the first example of a molecular adjuvant targeting a defined PRR approved for use in human vaccines (5). The development of immunomodulators

capable of stimulating additional PRR pathways offers the possibility of tuning immune responses to achieve appropriate protective immune responses to poorly immunogenic subunit antigens.

Recently, much attention has focused on cytosolic danger sensors and, particularly, the cytosolic nucleotide sensor stimulator of IFN genes (STING). STING, which localizes to the endoplasmic reticulum, is a potent inducer of type I IFNs in response to sensing cyclic dinucleotides (CDNs) (6). The CDNs recognized by STING are small-molecule second messengers used by all phyla of bacteria (7) and are also produced as endogenous products of the cytosolic DNA sensor cyclic GMP-AMP synthase (8–10). The canonical bacterial CDN, cyclic di-GMP (cdGMP), has been shown to directly bind STING and subsequently initiate IRF3- and NF- $\kappa$ B-dependent immune responses (11–13).

In parallel to these structural and molecular biology studies defining the pathways by which CDNs stimulate innate immunity, chemically synthesized CDNs, including cdGMP, cyclic di-inosine monophosphate, and cyclic di-AMP, are beginning to be explored as possible adjuvants for subunit vaccines, with particular success in promoting mucosal immunity to intranasal vaccines (6, 14–16). While these early studies point to the potential of CDNs as adjuvants promoting both T cell and humoral responses to subunit vaccines, the potency of STING agonists as parenteral adjuvants for systemic immunity remains unclear. For example, while vaccines administered with modest doses of cdGMP (5  $\mu$ g) have been reported to elicit substantial antibody titers in response to highly immunogenic model antigens, such as ovalbumin (OVA) or  $\beta$ -galactosidase (15, 17, 18), this same

**Conflict of interest:** The authors have declared that no conflict of interest exists.

**Submitted:** November 14, 2014; **Accepted:** April 2, 2015.

**Reference information:** *J Clin Invest.* 2015;125(6):2532–2546. doi:10.1172/JCI79915.

dose of cdGMP administered with hemagglutinin protein as a clinically relevant influenza antigen was completely ineffective as a parenteral vaccine (19). Similarly, cdGMP administered s.c. with HIV pseudovirions was also ineffective at adjuvanting humoral responses against the HIV Env protein (20). Karaolis and colleagues reported that parenteral (i.m.) vaccination with cdGMP adjuvanted humoral responses to the *Staphylococcus aureus* clumping factor A antigen, but much higher doses of CDN (145  $\mu$ g) were used (21). Parenteral immunization with 70 to 290  $\mu$ g cdGMP and hepatitis B surface antigen similarly elicited robust humoral responses, but this response was also accompanied by substantial inflammatory cytokine and chemokine production in the systemic circulation 24 hours after immunization (22). Such systemic inflammatory signatures are problematic for prophylactic vaccines and are likely due to systemic dissemination of these low-molecular-weight adjuvants, as has been seen with other small-molecule adjuvants, such as resiquimod (R848) (23). Altogether, these reports suggest that CDNs may be effective adjuvants for weakly immunogenic antigens but that finding an acceptable balance between potency and toxicity may be challenging for unformulated CDNs (24).

An effective strategy to simultaneously enhance the potency and safety of molecular adjuvants is to formulate these compounds in carriers such as nanoparticles. Nanoparticle vehicles, such as polymer particles or liposomes, can promote adjuvant transport through lymphatics to draining lymph nodes (dLNs), while blocking dissemination into the systemic circulation (25, 26). Concentration of molecular adjuvants in lymph nodes (LNs) using nanoparticle carriers can enable profound dose sparing of molecular adjuvants, and this approach has been demonstrated for a number of TLR agonists, including MPLA, CpG DNA, poly(I:C), and small-molecule TLR7/8 compounds (27–33). Importantly, a number of TLR agonist-carrying particle formulations have been demonstrated to effectively adjuvant the immune response when simply admixed with particulate or soluble antigen, i.e., without requiring incorporation of antigen and adjuvant together in particles (32, 34–36). Liposomal and oil-based nanoparticle emulsions carrying TLR agonists have also been shown to be effective in early-stage clinical trials (5, 37, 38).

Motivated by these findings, here we tested the hypothesis that concentration of CDNs within lymphoid tissues through the use of a nanoparticle carrier could both enhance their relative potency and decrease systemic inflammatory side effects, providing a means to exploit STING signaling for enhanced cellular and humoral immunity without toxicity. Using a liposomal nanoparticle formulation of cdGMP, we found that efficient lymphatic delivery of CDNs has a broad impact on both innate and adaptive immune responses, including potent activation of antigen-presenting cells (APCs), expansion of vaccine-specific helper T cells, and robust induction of germinal center B cell differentiation. These cellular responses to nanoparticle-CDN vaccination correlated with strong and durable vaccine-specific antibody induction equivalent to approximately 30-fold higher doses of soluble CDNs, without the systemic inflammatory toxicity of the latter. These enhancements in humoral immunity achieved by nanoparticle-delivered CDN adjuvants were dependent on TNF- $\alpha$  signaling but not type I IFNs.

## Results

**Lipid nanoparticles concentrate cdGMP in LN APCs.** In preliminary studies, we confirmed that, as reported for other antigens (19, 20), modest doses (5  $\mu$ g) of cdGMP administered with weakly immunogenic proteins (e.g., HIV gp120) or low doses of highly immunogenic antigens like OVA were ineffective for adjuvanting humoral responses above those of protein alone following parenteral immunization (data not shown). To determine whether this lack of efficacy reflected insufficient transport of CDNs to dLNs, we assessed LN accumulation of cdGMP following s.c. injection, using a fluorophore-conjugated derivative to enable detection of cdGMP in the tissue. As shown in Figure 1A, CDN levels in the dLNs remained <4 ng/mg tissue at all time points after injection of unformulated cdGMP. By flow cytometry, cdGMP fluorescence was undetectable above background in B220<sup>+</sup> B cells, CD11c<sup>+</sup>CD8 $\alpha$ <sup>+</sup> DCs, or CD11c<sup>+</sup>CD8 $\alpha$ <sup>-</sup> DCs and only found in 2.1%  $\pm$  2.6% of macrophages (identified as NK1.1<sup>-</sup>CD11c<sup>-</sup>CD11b<sup>+</sup>Ly6G<sup>-</sup>SSC<sup>lo</sup> cells, ref. 39 and Supplemental Figure 1; supplemental material available online with this article; doi:10.1172/JCI79915DS1) from inguinal or axillary LNs (Figure 1, B and C). Inefficient capture of cdGMP in the LNs is consistent with the low molecular weight of CDNs, which will be capable of absorption directly into blood capillaries at the injection site. Indeed, measurement of cdGMP in the blood showed rapid systemic dissemination of the soluble CDN following injection (Figure 1A).

Both the potency and safety of CDNs as candidate adjuvant compounds should be enhanced by concentration in local lymphoid tissues. We thus developed a liposomal nanoparticle formulation of cdGMP to enhance the delivery of these compounds to lymphatics and promote their capture in dLNs by APCs. cdGMP was encapsulated in 150 nm phosphatidylcholine liposomes containing 5 mol% of a PEGylated lipid; PEG reduces nonspecific interactions of the vesicles with serum proteins/matrix, enabling better retention of encapsulated drugs (40), and modestly enhances lymphatic uptake of liposomes (41, 42). PEGylated lipid nanoparticles loaded with fluorescently labeled cdGMP were relatively stable in serum, releasing only 4% of the encapsulated CDN when incubated in the presence of 10% serum at 37°C for 3 days (Figure 1D). In vitro, DCs internalized cdGMP in soluble or nanoparticle forms to equivalently high levels (Figure 1E). However, in contrast to the results with free CDN, s.c. injection of nanoparticle-cdGMP (NP-cdGMP) led to substantial accumulation of the STING agonist in the dLNs, peaking at approximately 60 ng/mg tissue at 24 hours (15-fold greater than unformulated CDN) and slowly decaying over the subsequent 2 days (Figure 1A). At 24 hours after injection, particle-delivered cdGMP was detected in approximately 8% of LN macrophages and 3% to 4% of CD8 $\alpha$ <sup>-</sup> and CD8 $\alpha$ <sup>+</sup> DCs, but with little uptake observed in B cells (Figure 1, B and C). To track the kinetics of lipid nanoparticle uptake by DCs over time, we encapsulated fluorescent OVA (OVA<sub>AF647</sub>) in the particles as a bright tracer, coinjected a 50:50 mixture of NP-cdGMP and NP-OVA<sub>AF647</sub>, and analyzed the frequency of NP-OVA<sub>AF647</sub><sup>+</sup> cells in dLNs over time. As shown in Figure 1F, the frequency of NP<sup>+</sup>CD8 $\alpha$ <sup>+</sup> DCs remained relatively constant over 2 days, but NP<sup>+</sup>CD8 $\alpha$ <sup>-</sup> DCs continued to increase in frequency to a peak of approximately 8% at 48 hours before decaying. Coincident with increased delivery to LNs, nanoparticle delivery of cdGMP blocked dissemination of cdGMP into the systemic circulation (Figure 1A).

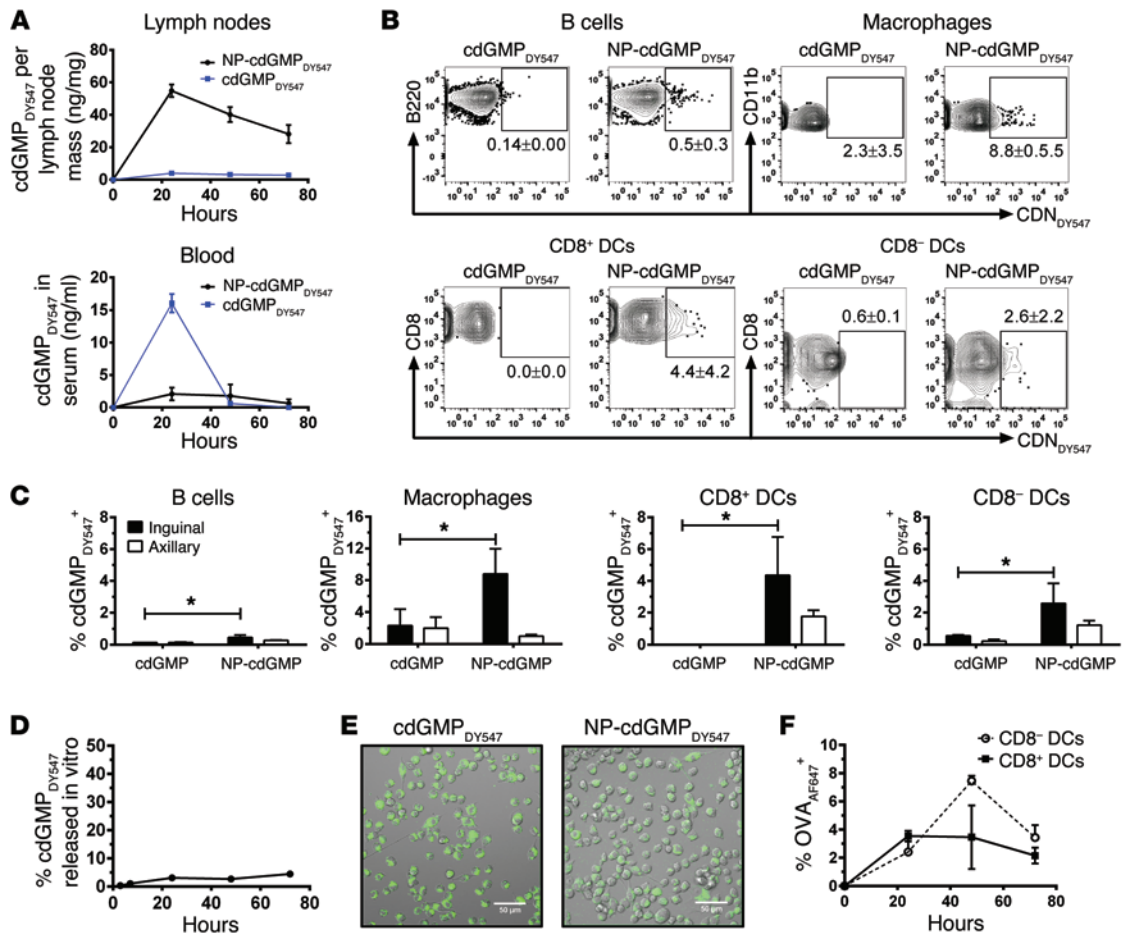


**Figure 1. NP-cdGMP enhances LN uptake of CDNs.** (A) Groups of BALB/c mice were injected with cdGMP<sub>DY547</sub>. The presence of CDN in dLNs (2 μg cdGMP<sub>DY547</sub> per mouse, n = 3 per group) and sera of these animals (5 μg cdGMP<sub>DY547</sub> per mouse, n = 5 per group) was traced by fluorescence spectroscopy. (B) Representative flow cytometry plots of CDN fluorescence in APCs 24 hours following s.c. injection of 2 μg cdGMP<sub>DY547</sub> or NP-cdGMP<sub>DY547</sub>. (C) Mean percentages of cdGMP<sub>DY547</sub><sup>+</sup> APCs in inguinal or axillary LNs at 24 hours after immunization of NP-cdGMP<sub>DY547</sub> or soluble cdGMP<sub>DY547</sub> (n = 3 per group). \*P < 0.05, ANOVA followed by Tukey's multiple comparison test. (D) Kinetics of cdGMP<sub>DY547</sub> release from nanoparticles incubated in PBS containing 10% serum at 37°C. (E) Representative images of DC2.4 cells after 2-hour incubations with NP-cdGMP<sub>DY547</sub> or soluble cdGMP<sub>DY547</sub>. Scale bar: 50 μm. (F) Percentage OVA<sub>AF647</sub><sup>+</sup> DCs over time following injection of NP-cdGMP and NP-OVA<sub>AF647</sub> (n = 4 per group).

*NP-cdGMP is a potent immunotherapeutic adjuvant.* cdGMP has been reported to have antitumor activity in murine cancer models (43, 44), likely due to the ability of type I IFN to enhance CD8<sup>+</sup> T cell responses during cross-priming (45). To first measure the impact of nanoparticle delivery on T cell priming, C57BL/6 mice were immunized with OVA protein alone or adjuvanted by 5 μg cdGMP in soluble or nanoparticle form. Intracellular cytokine staining was performed at 7 days after boost on peripheral blood mononuclear cells (PBMCs) restimulated with the immunodominant CD4<sup>+</sup> and CD8<sup>+</sup> T cell epitopes from OVA to identify cytokine-producing antigen-specific T cells. NP-cdGMP-adjuvanted vaccines induced 4-fold and 3-fold greater total cytokine<sup>+</sup> CD8<sup>+</sup> and CD4<sup>+</sup> T cell frequencies, respectively, compared with vaccination with soluble CDN adjuvant, and increased the frequency of polyfunctional (IFN-γ<sup>+</sup>TNF-α<sup>+</sup>) cells by 5-fold (Figure 2A). To assess the functional efficacy of these T cell responses in a therapeutic setting, we tested the capacity of NP-cdGMP to promote antitumor immunity against OVA- or self-antigen-expressing tumors. Mice with established EG.7-OVA tumors were vaccinated

on days 6, 13, and 20 with 10 μg OVA with or without 5 μg cdGMP. On day 19, the frequency of circulating OVA-specific CD8<sup>+</sup> T cells was measured by flow cytometry analysis of SIINFEKL peptide/MHC tetramer-binding cells among PBMCs. NP-cdGMP vaccines induced nearly 3-fold higher frequencies of antigen-specific CD8<sup>+</sup> T cell responses compared with soluble cdGMP (Figure 2, B and C). More strikingly, while soluble cdGMP-adjuvanted vaccines had little impact on tumor growth or animal survival, NP-cdGMP vaccination controlled tumor growth and induced greatly prolonged survival, as shown in Figure 2, D and E. To test a more aggressive tumor model with a vaccine targeting a tumor-associated antigen, animals were inoculated with B16F10 melanoma cells s.c. and vaccinated 3 times, beginning on day 5, with a gp100 lipopeptide (46) adjuvanted by soluble or nanoparticle cdGMP. NP-cdGMP enhanced the frequency of gp100-specific CD8<sup>+</sup> T cells by 7-fold compared with soluble cdGMP vaccines, delayed tumor growth, and prolonged animal survival (Supplemental Figure 3).

*NP-cdGMP induces type I IFN directly in LNs and elicits greater APC activation than soluble CDN.* To determine the impact of

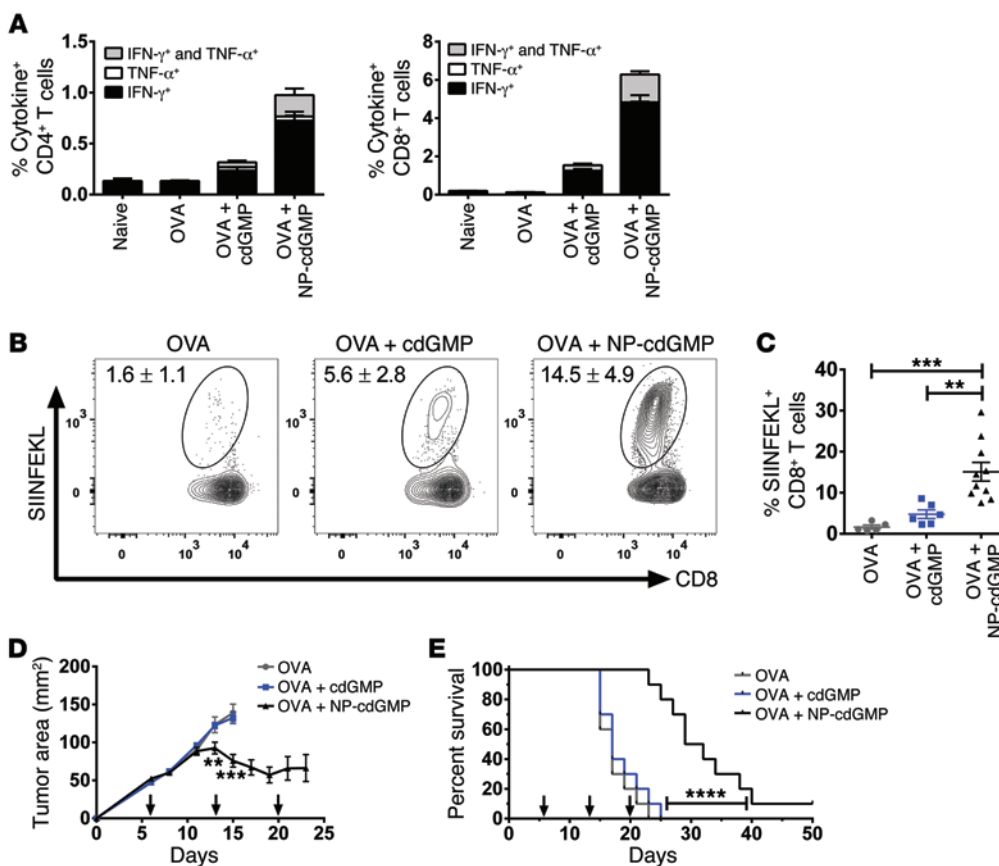


**Figure 2. NP-cdGMP promotes potent CD8<sup>+</sup> T cell responses and therapeutic antitumor immunity.** (A) C57BL/6 mice were immunized with 10  $\mu$ g OVA alone or OVA mixed with 5  $\mu$ g cdGMP or 5  $\mu$ g NP-cdGMP on days 0 and 14. On day 21, PBMCs were restimulated ex vivo with immunodominant CD4<sup>+</sup> and CD8<sup>+</sup> OVA epitopes and analyzed by flow cytometry for intracellular cytokine staining. Mean single- and double-cytokine<sup>+</sup> cell frequencies from each group are shown. (B–E) C57BL/6 mice ( $n = 10$  per group) were inoculated with  $1 \times 10^6$  EG.7-OVA cells s.c. on day 0 and then vaccinated with 10  $\mu$ g OVA alone or OVA mixed with 5  $\mu$ g cdGMP or 5  $\mu$ g NP-cdGMP on days 6, 13, and 20. (B) Representative flow cytometry plots. (C) Mean percentages of SIINFEKL-tetramer<sup>+</sup> CD8<sup>+</sup> T cells on day 19. (D) Tumor size over time (compared with OVA alone). (E) Survival over time. \*\* $P < 0.01$ ; \*\*\* $P < 0.001$ ; \*\*\*\* $P < 0.0001$ , 1-way ANOVA (C),  $t$  test (D), and log-rank Mantel-Cox test (E).

enhanced LN delivery on APC activation and humoral immune responses, we evaluated CDNs as adjuvants for a poorly immunogenic vaccine antigen, the membrane proximal external region (MPER) from HIV gp41. The MPER antigen, which as part of the HIV envelope trimer is thought to reside in juxtaposition to the viral membrane (47, 48), was formulated as a palmitoyl-anchored peptide displayed on the surface of liposomes that also contained a helper epitope derived from gp120 (denoted herein as HIV30; ref. 49) tethered by PEG to the inner leaflet of the vesicles (Figure 3A). We have previously shown that this nanoparticle MPER formulation (NP-MPER) elicits extremely weak anti-MPER humoral responses in the absence of coadministered molecular adjuvants (50). Thus, we compared NP-MPER vaccines adjuvanted with soluble cdGMP or NP-cdGMP (Figure 3A).

We first assessed the activation of APCs in dLNs after cdGMP/NP-MPER immunizations. Twenty hours after vaccination with NP-MPER and NP-cdGMP, both CD86 and MHC-II were strongly upregulated on CD8 $\alpha$ <sup>+</sup> and CD8 $\alpha$ <sup>-</sup> DCs (Figure 3, B and C), while vaccination with NP-MPER and soluble cdGMP elicited much weaker CD86 and MHC-II expression. CD86 and

CD69 were also upregulated on a large proportion of B cells following NP-cdGMP immunization, while soluble cdGMP induced these activation markers on a minority of these cells (Figure 3D). Tracking the frequencies of CD86<sup>+</sup> APCs over time revealed distinct dynamics for APC activation induced by soluble versus nanoparticle cdGMP: DC activation was low and peaked at 48 hours following NP-MPER vaccination with soluble cdGMP as adjuvant. By contrast, vaccination with NP-cdGMP as adjuvant elicited approximately 4-fold higher frequencies of activated DCs, which remained elevated for 48 hours before decaying toward baseline (Figure 3E). In addition, the peak frequency of macrophage activation was 3-fold higher after NP-cdGMP-adjuvanted vaccination than after soluble cdGMP-adjuvanted vaccination. As expected, non-adjuvanted NP-MPER vaccines elicited lower frequencies of activated APCs than either of the cdGMP-adjuvanted groups.

The induction of activation markers on a majority of LN APCs following NP-cdGMP immunization indicated that many more APCs were activated than directly acquired cdGMP, indicating strong *in trans* activation of B cells and DCs by cdGMP<sup>+</sup> cells. To distinguish between direct action of CDNs locally in dLNs and stimulation of LNs remotely via cytokines produced at the vaccine injection site, we evaluated the expression of IFN- $\beta$ , a signature product of STING activation by cdGMP (51, 52). RT-PCR analysis of dLNs showed that immunization with NP-MPER and NP-cdGMP induced robust expression of both *Ifnb1* and its downstream gene target *Rsad2* that peaked 20 hours after injection, reaching 35-fold higher levels relative to soluble cdGMP vaccination (Figure 3F). Nonadjuvanted vaccines showed minimal IFN- $\beta$  expression at all time points studied. Thus, concentration of CDNs in LNs by nanoparticle delivery induced a much greater frequency of activated APCs and higher expression of activation markers on a per-cell basis compared with vaccination with unformulated CDNs, which correlated with evidence for direct activation of type I IFN expression in LNs by the nanoparticle formulation.

*Nanoparticle delivery of cdGMP enhances expansion of helper T cells and promotes germinal center induction.* Follicular helper T cells (T<sub>fh</sub> cells) provide critical signals to germinal center B cells

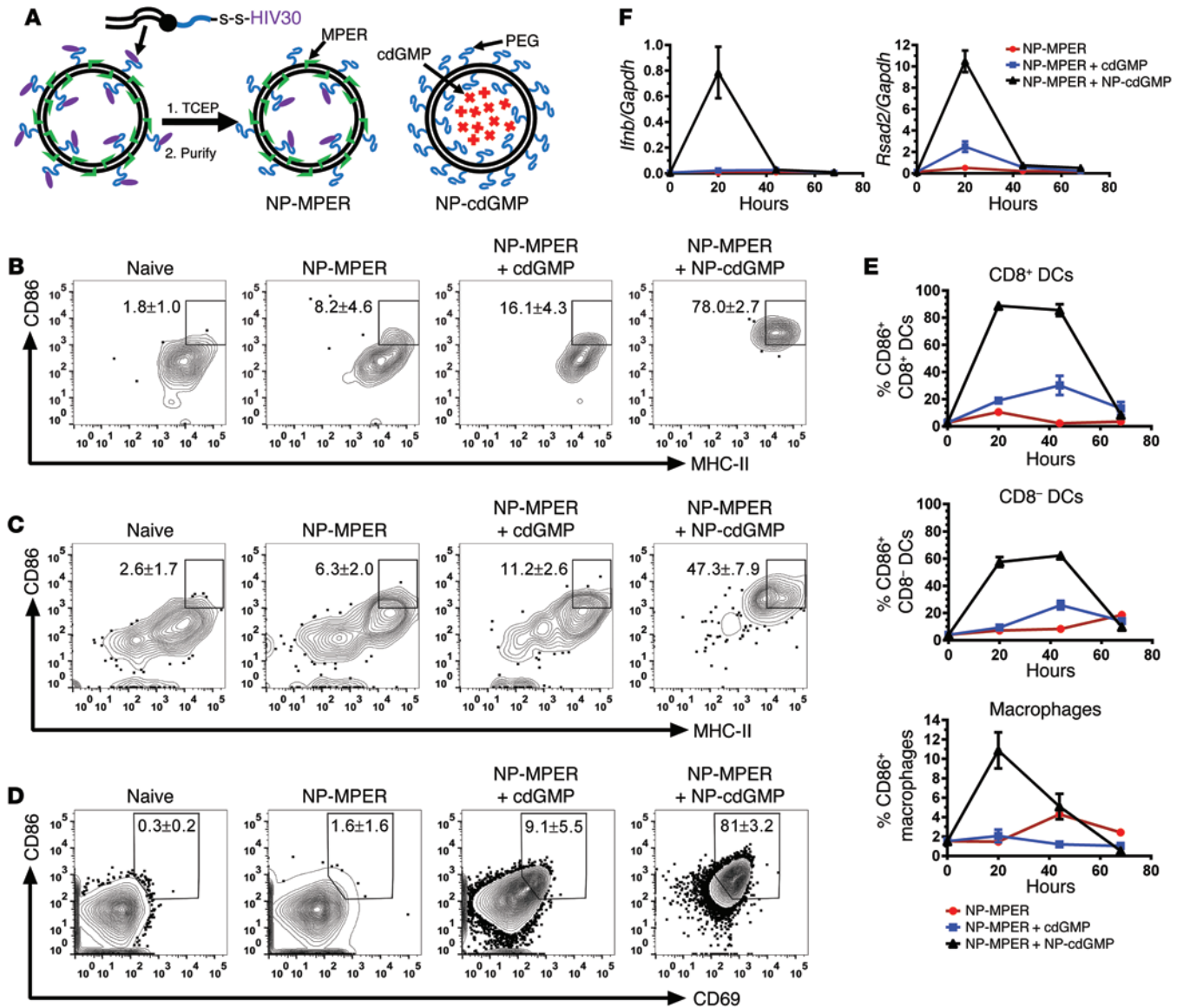


**Figure 3. NP-cdGMP potently activates APCs.** (A) Schematic of NP-MPER and NP-cdGMP vaccine. TCEP, Tris [2-carboxyethyl] phosphine. (B–F) BALB/c mice ( $n = 4$  per group) were immunized with NP-MPER alone, NP-MPER plus  $5 \mu\text{g}$  cdGMP, or NP-MPER plus  $5 \mu\text{g}$  NP-cdGMP, and dLNs were collected 20, 42, or 68 hours later for analysis. (B) Representative flow cytometry data for CD86 and MHC-II expression on CD8 $\alpha^+$ CD11c $^+$  cells, (C) CD8 $\alpha^-$ CD11c $^+$  cells, and (D) B220 $^+$  B cells. Gates are annotated with mean frequency  $\pm$  SD for each group. (E) Percentage CD86 $^+$  APC populations as a function of time. Representative data from 1 of 2 independent experiments are shown. (F) Expression levels of *Ifnb* and *Rsad2* over time in dLNs, as determined by RT-PCR.

in support of humoral immunity (53). To test the impact of cdGMP adjuvants on the expansion of vaccine-specific helper T cells and Tfh cell differentiation, we used an adoptive transfer model using OVA-specific OT-II TCR-transgenic CD4 $^+$  T cells and liposomal MPER vaccines, incorporating the OT-II cognate peptide antigen instead of HIV30 as a helper epitope. CD90.1 $^+$  OT-II CD4 $^+$  T cells were adoptively transferred into C57BL/6 recipients, which were immunized 24 hours later with NP-MPER vaccines carrying the OT-II epitope with or without addition of cdGMP or NP-cdGMP. One week after immunization, animals were sacrificed for flow cytometry analysis. As shown in Figure 4A, immunization with liposomes lacking T helper peptide or using soluble cdGMP adjuvant failed to significantly expand OT-II $^+$  cells compared with

unadjuvanted liposomes. By contrast, vaccination with NP-MPER/OT-II and NP-cdGMP induced a substantial expansion of the transferred OVA-specific T cells, with 5.1-fold more OT-II $^+$  cells recovered on day 7 compared with soluble cdGMP-adjuvanted vaccines (Figure 4, A and B). The greater increase in T cell expansion for NP-cdGMP seen in total cell counts compared with cell frequencies was a result of substantially greater LN swelling and total LN cell numbers in NP-cdGMP-vaccinated mice (data not shown). The frequency of antigen-specific T cells differentiating to a CXCR5 $^+$ PD-1 $^+$  follicular helper phenotype was only slightly greater for NP-cdGMP- vs. soluble cdGMP-adjuvanted vaccines (Figure 4C), but the much greater overall expansion of the antigen-specific T cell population after administration of the former vac-

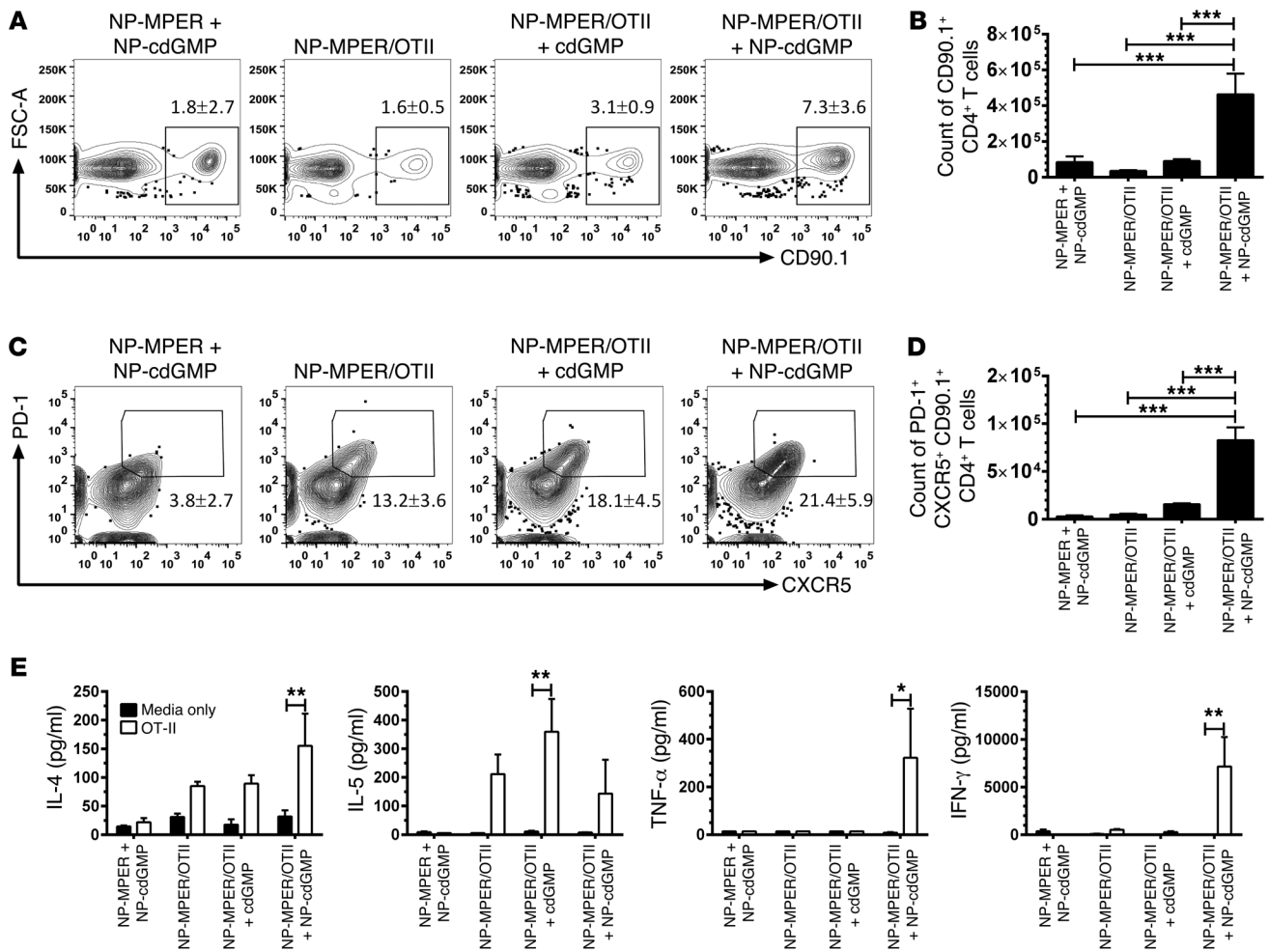


**Figure 4. NP-cdGMP promotes antigen-specific CD4<sup>+</sup> T cell expansion.** (A–D) C57BL/6 mice ( $n = 4$  per group) received adoptive transfer of  $10^5$  CD90.1<sup>+</sup> OT-II CD4 T cells and were immunized 24 hours later with NP-MPER with or without the OT-II helper epitope and with or without addition of cdGMP or NP-cdGMP. One week later, OT-II T cell responses were characterized via flow cytometry. (A and C) Representative flow cytometry plots and (B and D) total cell counts of total CD90.1<sup>+</sup> OT-II T cells and CXCR5<sup>+</sup>PD-1<sup>+</sup> OT-II cells, respectively. Data are combined from two independent experiments (in total  $n = 8$  mice per group). (E) C57BL/6 mice ( $n = 3$  per group) without OT-II adoptive transfer were immunized as in A on days 0, 21, and 42, and on day 49 splenocytes were restimulated for 48 hours with OT-II peptide or media only, and supernatants were assessed for cytokines by bead-based ELISA. \* $P < 0.05$ ; \*\* $P < 0.01$ ; \*\*\* $P < 0.001$ , ANOVA followed by Tukey’s multiple comparison test (B and D) and Bonferroni’s multiple comparison test (E).

cines led to 5.3-fold more OT-II Tfh cells (Figure 4D). In parallel, we assessed endogenous T cell responses to NP-MPER/OT-II and CDN vaccines in C57BL/6 mice (with no adoptive transfers). Splenocytes from all of the vaccine groups that received helper peptide produced IL-4 and IL-5 when restimulated with OT-II peptide *ex vivo*, but only animals vaccinated with NP-cdGMP as adjuvant also produced IFN- $\gamma$  and TNF- $\alpha$  (Figure 4E).

Given the enhanced expansion of follicular helper cells stimulated by NP-cdGMP, we next examined B cell differentiation and germinal center induction following CDN-adjuvanted immunizations. Groups of mice were immunized with NP-MPER with or without cdGMP adjuvants, and 8 days after immunization, B cell differentiation in dLNs was analyzed via flow cytometry. None of these primary NP-MPER immunizations induced substantial plasmablast differentiation (Figure 5, A and B). However, germinal center induction was strongly affected by NP-cdGMP adjuvants; mice that received NP-MPER and NP-cdGMP immunization

showed greatly increased numbers of PNA<sup>+</sup>GL-7<sup>+</sup> germinal center B cells (Figure 5, C and D).

*cdGMP nanoparticles promote strong humoral responses, while avoiding systemic cytokine induction.* To confirm that cdGMP acts in a STING-dependent manner when delivered in nanoparticles, wild-type (C57BL6/J) or STING-deficient (C57BL/6J-Tmem173gt/J, golden ticket mutation) mice (54) were immunized with NP-MPER and NP-cdGMP. As expected, MPER-specific antibody responses promoted by NP-cdGMP were dependent on the presence of STING (Figure 6A). To determine the impact of enhanced helper T cell expansion and germinal center induction by NP-cdGMP on the humoral immune response, we next assessed antibody titers elicited by CDN-adjuvanted vaccines. To address relative potency of the soluble and formulated CDNs, NP-MPER vaccines were administered as a prime and boost with 5  $\mu$ g NP-cdGMP and compared with vaccines adjuvanted by soluble cdGMP in doses ranging from 5 to 150  $\mu$ g. NP-cdGMP-adjuvanted vac-

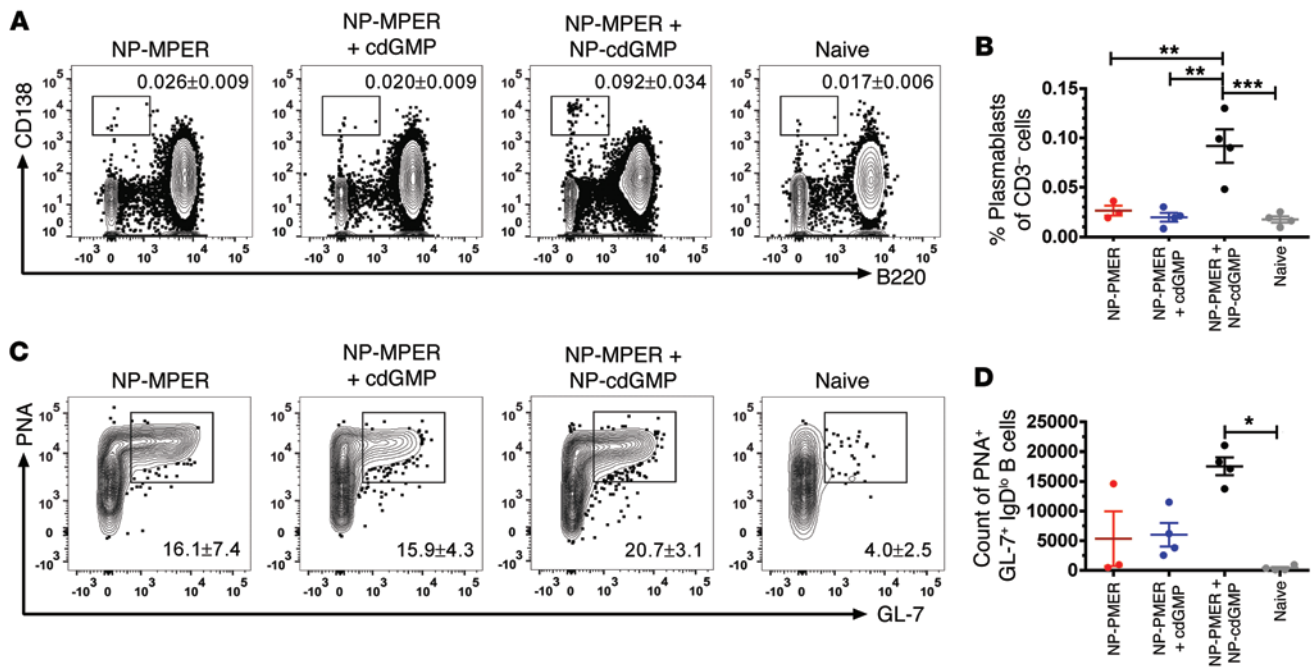


**Figure 5. Primary plasmablast and germinal center formation is enhanced with NP-cdGMP.** BALB/c mice ( $n = 4$  per group) were immunized with NP-MPER/HIV30 alone or adjuvanted with  $5 \mu\text{g}$  cdGMP or NP-cdGMP. dLNs were collected 8 days after immunization for analysis via flow cytometry. (A) Representative flow cytometry plots and (B) frequencies of  $\text{CD138}^+\text{B220}^+\text{CD3}\epsilon^-$  plasmablasts. (C) Representative flow cytometry plots and (D) cell counts of  $\text{GL-7}^+\text{PNA}^+\text{IgD}^{\text{lo}}\text{B220}^+$  germinal center B cells. (D) Cell counts of germinal center B cells.  $*P < 0.05$ ;  $**P < 0.01$ ;  $***P < 0.001$ , ANOVA followed by Tukey's multiple comparison test.

cines elicited 8.2-fold higher levels of total anti-MPER serum IgG than the equivalent soluble cdGMP dosage, and 50% of animals immunized with soluble cdGMP failed to mount any detectable IgG response at this dose of cdGMP (Figure 6B). NP-cdGMP similarly elicited enhanced MPER-specific IgG1 and IgG3 responses. Increasing the dose of unformulated cdGMP led to increasing MPER-specific IgG responses, but only the highest dose of soluble cdGMP ( $150 \mu\text{g}$ ) elicited antibody titers comparable to the nanoparticle CDN formulation (Figure 6B). However, measurement of serum inflammatory cytokines 6 hours after immunization revealed that this roughly equipotent dose of soluble cdGMP elicited much higher levels of systemic IL-6, TNF- $\alpha$ , and IFN- $\beta$  than NP-cdGMP immunization (Figure 6C), with the latter suggesting systemic triggering of STING. Thus, nanoparticle-mediated concentrations of cdGMP in LNs enabled robust humoral immune responses to a poorly immunogenic vaccine to be achieved, without concomitant induction of systemic inflammatory toxicity.

We next assessed the durability of humoral responses elicited by CDN adjuvants and compared their potency to MPLA, a well-studied and effective adjuvant for humoral immunity representative of the TLR4 agonist adjuvants in several licensed vaccines (5, 55). Mice were immunized on days 0, 21, and 42 with NP-MPER alone, NP-MPER with coinorporated MPLA, or NP-MPER adjuvanted by cdGMP or NP-cdGMP. Peak antibody titers 7 days after the second boost were 11-fold greater for vaccines adjuvanted by NP-cdGMP compared with those adjuvanted by either soluble cdGMP or MPLA (Figure 7A). Antibody isotype analysis demonstrated that NP-cdGMP-adjuvanted vaccines consistently induced 20- to 100-fold higher MPER-specific IgG1, IgG2A, and

IgG3 responses compared with soluble cdGMP- or MPLA-adjuvanted vaccines (Figure 7B). Further, at 4.5 months after priming, MPER titers elicited by the MPLA-adjuvanted vaccine had waned by 40%, while vaccines administered with NP-cdGMP showed no decay in total serum MPER-specific IgG (Figure 7A). Even following two booster immunizations, vaccines adjuvanted by NP-cdGMP trended toward higher frequencies of germinal center cells in LNs compared with vaccines adjuvanted by NP-MPER/MPLA or NP-MPER and cdGMP (Figure 7C). Because distinct danger signal pathways can act in synergy (56, 57), we also evaluated the relative effectiveness of MPER-NP vaccines adjuvanted with both MPLA and cdGMP. Addition of soluble cdGMP to MPLA/MPER-NP vaccines increased their post boost peak titer by 5.3-fold, while the addition of NP-cdGMP to the MPLA/MPER-NP vaccine increased peak anti-MPER IgG responses 67-fold, a response that remained approximately 10-fold above titers elicited by MPLA-only-adjuvanted vaccines for at least 150 days (Figure 7D). This same trend of enhancement was also observed in IgG1, IgG2A, and IgG3 titers at day 49 (Figure 7E). Thus, CDNs promoted durable antibody responses, and even when compared with another nanoparticle-formulated molecular adjuvant (liposomal MPLA), NP-cdGMP elicited 11-fold greater steady-state antibody titers, which could be further modestly boosted by combining MPLA and CDNs as tandem adjuvants.

*CDN targeting to LNs ablates plasmacytoid DCs, but vaccine responses are independent of plasmacytoid DCs.* Although plasmacytoid DCs (pDCs) are both major producers of type I IFN and activated by IFNs (58, 59), it is unknown how CDNs affect pDCs and whether they play a role in the adjuvant activity of CDNs in

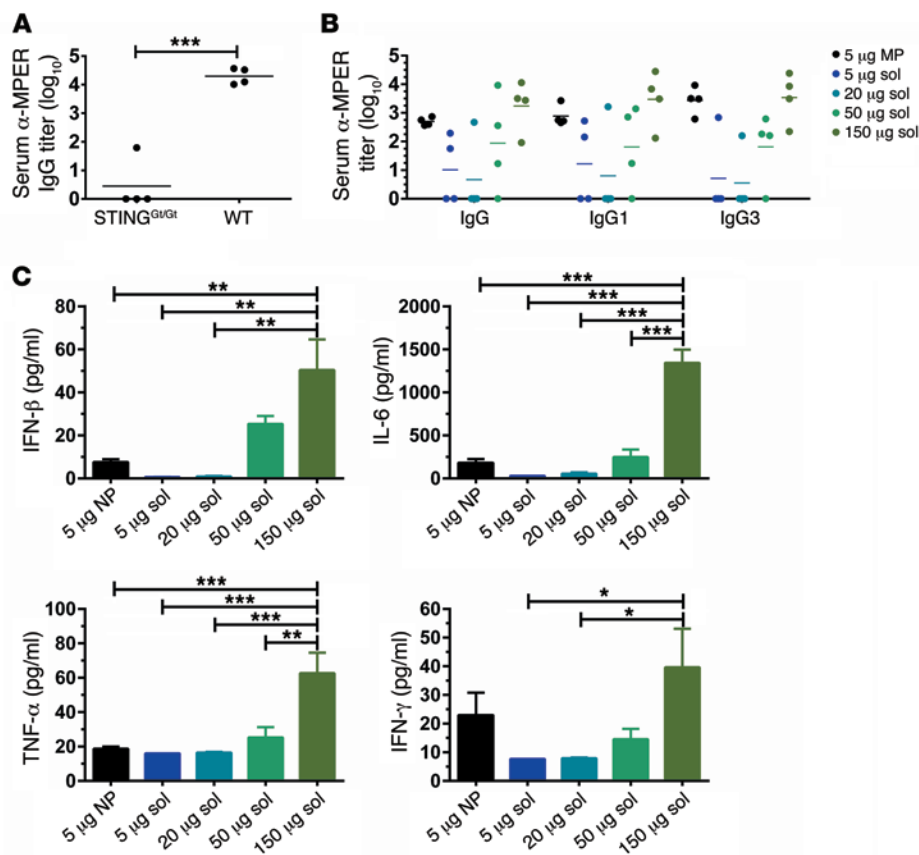


**Figure 6. NP-cdGMP promotes robust humoral immunity, while minimizing systemic cytokine induction.** (A) C57BL/6J (wild-type) or C57BL/6J-Tmem173gt/J (STING<sup>Gt/Gt</sup>, golden ticket mutation) mice were immunized on days 0 and 21 with NP-MPER/HIV30 plus NP-cdGMP ( $n = 4$  per group). Total serum anti-MPER IgG titers were assessed by ELISA on day 28. \*\*\* $P < 0.001$ , t test. (B and C) BALB/c mice ( $n = 4$  per group) were immunized on days 0 and 21 with NP-MPER/HIV30 combined with 5  $\mu$ g NP-cdGMP (NP) or graded doses of soluble cdGMP (sol). (B) ELISA analysis of serum anti-MPER IgG, IgG1 and IgG3 titers at day 28. (C) Serum cytokine levels assessed at 6 hours after immunization via ELISA. \* $P < 0.05$ ; \*\* $P < 0.01$ ; \*\*\* $P < 0.001$ , ANOVA followed by Turkey's multiple comparison test.

vivo. To investigate how LN targeting of cdGMP affected pDCs, mice were immunized with NP-MPER alone or with cdGMP adjuvants. dLNs were collected 1 day later, and B220<sup>+</sup>CD11c<sup>+</sup>PDCA1<sup>+</sup> pDCs were analyzed by flow cytometry (Supplemental Figure 2A). As shown in Figure 8, A and B, all of the immunizations induced an early decrease in the number of pDCs in dLNs, but cdGMP vaccines induced a remarkable sustained loss of these cells; pDCs were almost completely eliminated from dLNs of NP-cdGMP-immunized animals for several days. Quantification of pDC numbers in dLNs revealed that soluble cdGMP and NP-cdGMP rapidly induced 3-fold and 11-fold losses of pDCs compared with naive animals, respectively (Figure 8B). It has previously been shown that pDCs are engaged in an autocrine negative-feedback loop with type I IFN: during viral infections, pDCs produce large quantities of IFN, which in turn induces their apoptosis in an autocrine manner and transiently depletes these cells (60). However, the rapid loss of pDC populations by 20 hours following CDN-adjuvanted immunization suggests that these cells are not the source of the elevated levels of type I IFN expression detected in dLNs at this time point (Figure 3F). To confirm that pDCs were not playing an important role in the humoral response elicited by CDNs, mice were treated with a pDC-depleting antibody (or isotype control; Supplemental Figure 2B) and then immunized with NP-MPER and NP-cdGMP. Analysis of APC activation in dLNs indicated no difference in APC activation in pDC-depleted or control groups (Figure 8C). IgG antibody responses to the weakly immunogenic MPER peptide are weak to undetectable in the first 2 weeks after a single priming immunization, but responses against the HIV30 helper epitope cocarried by the liposomal vaccine were detectable

at day 14 after prime. Using these responses against the helper epitope as an early readout of the impact of pDC depletion on antibody production, we found that depletion of pDCs also had no effect on vaccine-specific antibody titers on day 14 (Figure 8D). Thus, pDCs do not appear to play an important role in the adjuvant activity of CDNs in the setting of parenteral immunization.

*Type I IFN and TNF- $\alpha$  play complementary roles following NP-cdGMP vaccination.* The discordance between the frequency of APCs directly taking up NP-cdGMP and the extent of APC activation elicited by this adjuvant suggests that cytokine signaling in *trans* plays a critical role in the adjuvant activity of CDN nanoparticles. Type I IFNs and TNF- $\alpha$  are major downstream products following cdGMP-induced activation of STING (14, 61), and given the strong upregulation of IFN- $\beta$  expression in LNs 20 hours after NP-cdGMP immunization, we first examined the role of type I IFN in the response to NP-cdGMP immunization. To test the role of type I IFN signaling, mice were administered a blocking anti-IFN- $\alpha/\beta$  receptor antibody (anti-IFN $\alpha$ R1) or its isotype control and then immunized with NP-MPER and NP-cdGMP. Twenty-four hours after immunization, animals treated with anti-IFN $\alpha$ R1 showed greatly reduced frequencies of CD86<sup>+</sup> B cells, macrophages, CD8 $\alpha$ <sup>+</sup> DCs, and CD8 $\alpha$ <sup>-</sup> DCs relative to the isotype control group (Figure 9A). However, this reduction in early APC activation had no influence on early antibody titers against the HIV30 helper peptide at day 14 (Figure 9B). Blaauboer et al. previously observed that antibody responses to mucosal vaccines adjuvanted with soluble cdGMP were independent of type I IFN but dependent on TNF- $\alpha$  (61). Although Blaauboer et al. used *Tnfr1*<sup>-/-</sup> mice to demonstrate the role of this cytokine on the adjuvant action of cdGMP,

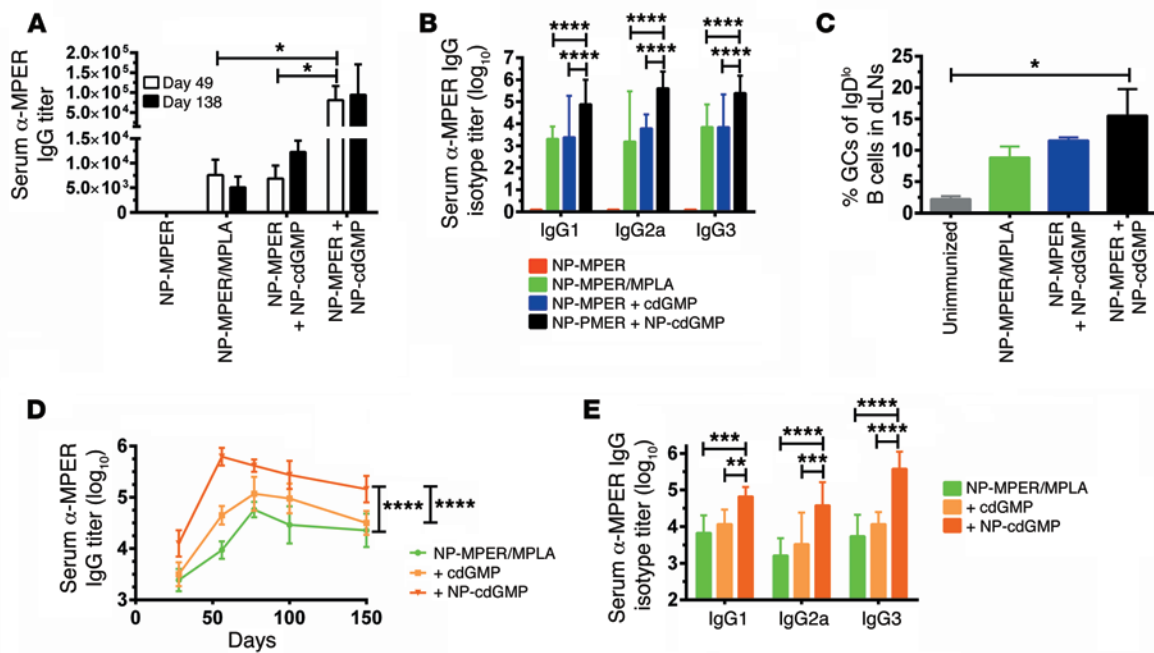


**Figure 7. NP-cdGMP elicits durable class-switched humoral responses and synergizes with MPLA to adjuvant MPER vaccines.** (A–C) BALB/c mice were immunized on days 0, 21, and 42 with NP-MPER/HIV30 alone, NP-MPER/HIV30/MPLA, or NP-MPER/HIV30 plus cdGMP or NP-cdGMP. (A) Serum anti-MPER total IgG titers assessed via ELISA on days 49 and 138 ( $n = 3$  per group).  $*P < 0.05$ , ANOVA followed by Tukey’s multiple comparison test. (B) ELISA analysis of specific isotypes of serum anti-MPER Ig at day 49 ( $n = 3$  per group).  $****P < 0.0001$ , ANOVA followed by Tukey’s multiple comparison test. (C) Percentages of PNA<sup>+</sup>GL-7<sup>+</sup>IgD<sup>+</sup>B220<sup>+</sup> germinal center B cells (GCs) in dLNs at day 49 ( $n = 3$  per group).  $*P < 0.05$ , ANOVA followed by Tukey’s multiple comparison test. Data from 1 representative of 2 independent experiments are shown. (D and E) BALB/c mice ( $n = 4$  per group) were immunized on days 0, 21, and 42 with NP-MPER/HIV30/MPLA alone or additionally adjuvanted with cdGMP or NP-cdGMP. (D) Serum anti-MPER IgG titers over time and (E) specific isotype responses at day 49 assessed via ELISA.  $P < 0.0001$ , comparison of NP-MPER/MPLA vs. NP-MPER/MPLA + NP-cdGMP groups over time.  $P < 0.0001$ , comparison of NP-MPER/MPLA + soluble cdGMP vs. NP-MPER/MPLA + NP-cdGMP over time, ANOVA followed by Tukey’s multiple comparison test.  $**P < 0.01$ ;  $***P < 0.001$ ;  $****P < 0.0001$ , ANOVA followed by Tukey’s multiple comparison test. Titer values in B and E show geometric mean and 96% confidence interval.

we chose to investigate this question by administration of an anti-TNF- $\alpha$  blocking antibody, due to the absence of follicular DC networks observed in *Tnfr1*<sup>-/-</sup> mice (62). Twenty-four hours after immunization with NP-MPER and NP-cdGMP, TNF- $\alpha$ -blocked mice exhibited marginal impairment in APC activation (Figure 9C), but at 2 weeks after prime, the TNF- $\alpha$  blockade reduced vaccine-specific antibody titers 115-fold (Figure 9D). Thus, cdGMP targeted to LNs via nanoparticle delivery acts through type I IFN and TNF- $\alpha$  to promote early APC activation and class-switched IgG production, respectively.

**Discussion**

CDNs are a relatively new class of immunomodulatory compounds with the potential to promote protective immunity through a unique pathway using the cytosolic danger sensor STING and its downstream transcription factors NF- $\kappa$ B and IRF-3 (6, 63). The publication of crystal structures demonstrating the structural basis for CDN sensing through STING (64, 65) and the identification of endogenous CDNs as signaling products produced by cyclic GMP-AMP synthase sensing of double-stranded DNA (9, 10, 66) have provided both a rationale and mechanistic guidance for the development of CDNs as adjuvants acting through type I IFNs and NF- $\kappa$ B activation in host cells. Indeed, several laboratories have recently demonstrated innate immune stimulatory (14, 22, 61) and adjuvant activities (63) with CDNs, particularly when applied

as mucosal adjuvants. For example, Ebensen et al. first demonstrated that intranasal administration of soluble antigen and cdGMP induced higher antigen-specific serum IgG and mucosal IgA when using the model antigen  $\beta$ -galactosidase (15). When administered intranasally with the *S. pneumonia* antigen pneumococcal surface protein A, cdGMP protected against *S. pneumonia* colonization (67). The ability of structurally related CDNs, such as cyclic di-inosine monophosphate and cyclic di-AMP, to adjuvant mucosal immunizations has also been reported (17, 68).

In contrast to the robust response to CDNs in mucosal immunization, the efficacy of CDNs as adjuvants in the setting of traditional parenteral immunization has been less clear, with much of the early published data focused on the use of CDNs to boost immunity against highly immunogenic model antigens and/or using large doses of CDNs. As shown here, the limited potency of parenterally administered CDNs reflects poor lymphatic uptake of these small-molecule immunomodulators; they are instead cleared from tissues via the blood. This biodistribution issue is a property of molecular size: because blood absorbs approximately 10-fold more fluid from tissues than lymph, molecules small enough to permeate blood vessels (less than ~1 kDa) tend to show predominant clearance to the blood (69). Therefore, increasing CDN-mediated vaccine responses through increased dosing of unformulated CDNs is accompanied by parallel increases in systemic inflammatory toxicity. This pharmacokinetic behavior is shared by other small-molecule

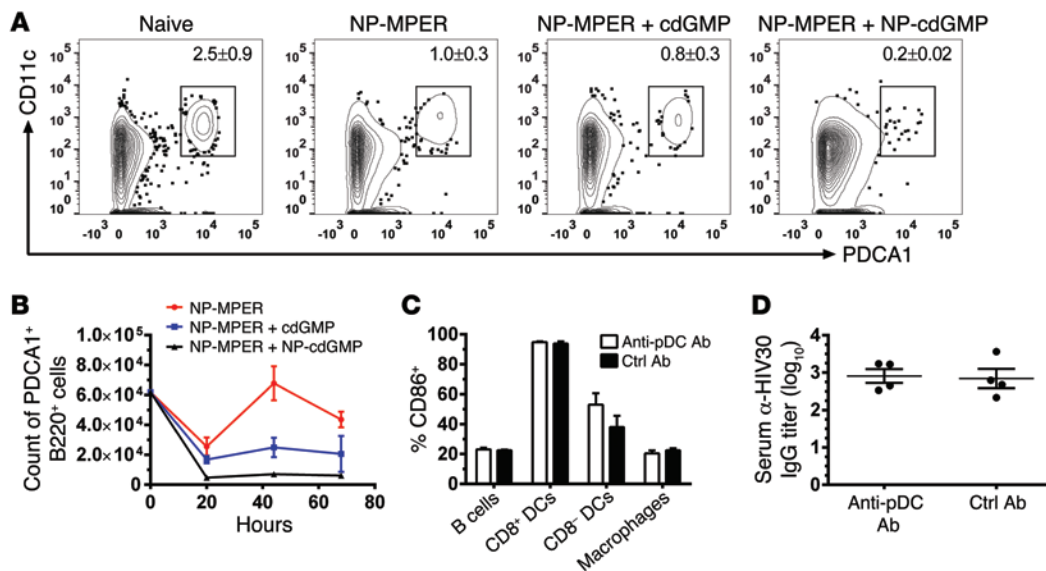


**Figure 8. NP-cdGMP-adjuvanted vaccine responses are independent of pDCs.** (A and B) BALB/c mice ( $n = 4$  per group) were immunized with NP-MPER alone or combined with cdGMP adjuvants. (A) Representative flow cytometry plots and (B) total cell counts of PDCA1<sup>+</sup>CD11c<sup>+</sup>B220<sup>+</sup> pDCs at 24 hours after immunization. Gates in A shown mean  $\pm$  SD percentages of pDCs. Data from 1 representative of 2 independent experiments are shown. (C and D) BALB/c mice ( $n = 4$  per group) were treated with pDC-depleting or isotype control antibodies and then immunized with NP-MPER/HIV30 and NP-cdGMP. (C) Mean percentage CD86<sup>+</sup> APCs at 20 hours after immunization. (D) Vaccine-specific anti-HIV30 antibody responses at 14 days after immunization.

adjuvant compounds, such as R848 and related imidazoquinoline TLR7/8 agonist compounds, muramyl dipeptides that trigger NLRs, and RNA oligonucleotide ligands of RIG-I (23, 70, 71). For example, parenteral injection of R848 is known to rapidly trigger systemic inflammatory cytokines, a phenomenon similar to the systemic signature observed here for CDNs, and induces transient systemic lymphopenia within hours of injection (36, 72). To overcome these issues, a number of strategies have been explored to limit systemic exposure and/or refocus molecular adjuvant delivery to LNs, including conjugating of adjuvant compounds with lipid tails (46, 72, 73), directly coupling to large-molecular-weight antigens (74, 75), or encapsulating in nano/microparticles (27, 30, 32, 36).

Here, we demonstrate that nanoparticle delivery using PEGylated liposomal carriers substantially enhances the potency of the canonical CDN cdGMP, eliciting enhanced CD4<sup>+</sup> and CD8<sup>+</sup> T cell responses to protein antigens and high-titer, durable humoral responses to a model weakly immunogenic peptide antigen at low doses of NP-cdGMP. These responses were only matched by approximately 30-fold higher doses of unformulated CDNs that may not be translatable to large animals or humans and that induced substantial systemic cytokine induction. This increase in potency was achieved by 15-fold increased LN NP-cdGMP accumulation relative to that after soluble cdGMP injection. NP-cdGMP was avidly pinocytosed/endocytosed by DCs *in vitro*, and despite the fact that these PEGylated nanoparticles were not designed to promote delivery of CDNs to the cytosol, we observed robust APC activation *in vivo*. However, it has recently been reported that STING is capable of sensing CDNs contained within impermeable vacuoles of host cells during *Chlamydia trachomatis* infection, and it is hypothesized that the ER wraps around the vacuole, enabling ER-localized STING to detect vacuole-entrapped cdGMP (76). Thus, APCs may harbor intrinsic mechanisms to sense endosomal CDNs.

Type I IFNs are signature downstream products of STING activation by CDNs in host cells (51, 52), and NP-cdGMP led to direct induction of type I IFN and downstream target gene expression in the dLNs. By contrast, soluble CDN administration induced no type I IFN in the dLNs, implying that its effects on APC activation are mediated by inflammatory cytokines produced at the injection site acting remotely on draining nodes. Such in *trans* activation of DCs by inflammatory cytokines has been shown to elicit weaker priming of T cell responses compared with *cis* activation of DCs directly through pathogen-sensing receptors (77, 78). Direct type I IFN induction in LNs by NP-cdGMP correlated with more robust upregulation of costimulatory and activation markers on LN APCs, which occurred earlier and was more sustained (over ~48 hours) compared with soluble CDN vaccination. Coincident with enhanced APC activation, NP-cdGMP drove a 5-fold increase in vaccine-specific CD4<sup>+</sup> T cell expansion compared with unformulated CDNs, increased CD8<sup>+</sup> T cell responses, and enhanced anti-tumor immunity in the setting of therapeutic vaccination. Thus, nanoparticle delivery of CDNs enhanced both early APC activation and subsequent T cell responses.

Our subsequent analyses focused on determining the impact of nanoparticle CDN delivery on humoral immunity, using a liposomal gp41 peptide as a model poorly immunogenic vaccine antigen. First, we examined the induction of antigen-specific follicular helper cells, because type I IFN induction in LNs by NP-cdGMP might be expected to drive Tfh differentiation (79). Nanoparticle delivery of cdGMP only moderately affected the frequency of CD4<sup>+</sup> T cells differentiating toward a follicular helper phenotype, but the much greater overall expansion of antigen-specific CD4<sup>+</sup> T cells by NP-cdGMP compared with soluble CDN adjuvants in turn translated into 5.3-fold more vaccine-specific Tfh cells. In line with their expected importance in class switching and germinal center forma-

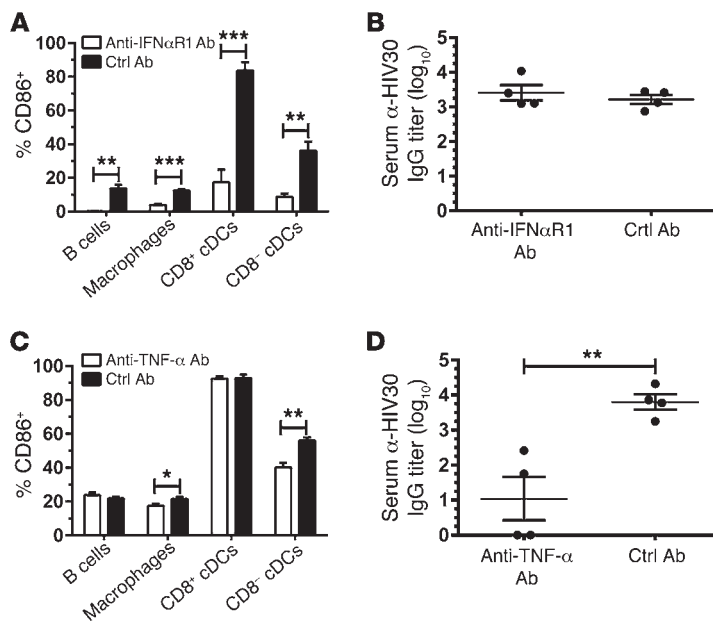


**Figure 9. Type I IFN shapes early activation of APCs, while TNF- $\alpha$  is critical for IgG production following cdGMP-adjuvanted immunization.** BALB/c mice ( $n = 4$  per group) were treated with anti-IFN $\alpha$ R1, anti-TNF- $\alpha$ , or respective isotype control antibodies and then immunized with NP-MPER/HIV30 and NP-cdGMP. **(A)** Percentages of CD86 $^+$  APCs in the presence of anti-IFN $\alpha$ R1 or isotype control antibody at 24 hours after immunization. Data from 1 representative of 2 independent experiments are shown. cDCs, conventional DCs. **(B)** Antigen-specific IgG titers at 14 days after immunization in the presence or absence of IFN $\alpha$ R1 blockade. **(C)** Percentages of CD86 $^+$  APCs in the presence of anti-TNF- $\alpha$  or isotype control antibody at 24 hours after immunization. **(D)** Antigen-specific IgG titers in the presence or absence of TNF- $\alpha$  blockade at 14 days after immunization. Data from 1 representative of 2 independent experiments are shown. \* $P < 0.05$ ; \*\* $P < 0.01$ ; \*\*\* $P < 0.001$ , individual  $t$  tests.

tion (53), increased numbers of specific Tfh were accompanied by enhanced germinal center B cell differentiation, 11-fold increased antigen-specific IgG titers that were dependent on the presence of STING, and humoral responses that were more durable than vaccines administered with the well-known TLR agonist MPLA. However, sera from these MPER-immunized animals did not neutralize HIV (data not shown), indicating that further structural refinements are required for this antigen to elicit antibodies capable of recognizing the functional stalk of the HIV envelope trimer (50).

The presence of IFN expression, suggesting STING activation directly in dLNs, led us to explore the source of type I IFNs following NP-cdGMP vaccination and to quantify the relative importance of the key downstream products of STING activation on the observed humoral responses. pDCs are major producers of type I IFN, but paradoxically these cells appeared to be strongly ablated following immunization with cdGMP. pDC depletion was detected by 20 hours after immunization, contemporaneous with peak IFN expression, suggesting that these cells are not the source of the type I IFN induced by NP-cdGMP. This finding is in agreement with a prior study reporting minimal human pDC activation by CDNs (14). In further support of the idea that pDCs do not play an important role in the adjuvant function of CDNs, pDC depletion had no impact on either early APC activation or subsequent IgG production following NP-cdGMP immunization. While type I IFNs are a characteristic product of STING activation, CDNs also trigger the production of TNF- $\alpha$  through NF- $\kappa$ B (52, 61). Both type I IFN and TNF- $\alpha$  have been shown to be important regulators of humoral immunity (80–82), but a recent study suggested that cdGMP applied intranasally adjuvants mucosal immunity in a type I IFN-independent, TNF- $\alpha$ -dependent manner (61). Here, we found that, following NP-cdGMP vaccination, both pathways of STING signaling are involved, with early APC activation dependent on IFN- $\alpha$  signaling and early (day 14) class-switched antibody responses dependent on TNF- $\alpha$ .

In the interest of translational relevance, we used a PEGylated liposome formulation with a composition similar in nature to that

of clinically approved liposomal drugs (83). A limitation of our bench-scale formulation approach was the relatively low CDN loading efficiency (~35%). However, more advanced polymer or lipid nanoparticle carriers (29, 84) that achieve more efficient drug loading and/or lipophilic modifications to CDNs to promote liposome association (a strategy used successfully with imidazoquinoline adjuvants; ref. 72) can readily be envisioned to circumvent this issue. Delivery of PRR agonists as adjuvants has variously been reported to require coencapsulation in the same particle as the antigen (*in cis*) (85) or simply simultaneous delivery on separate particles (*in trans*) (32, 36, 86). The ability of NP-cdGMP to adjuvant immune responses *in trans* to particulate antigen provides flexibility for vaccine production and facilitates inclusion of NP-cdGMP into existing vaccine platforms. Although many danger signals are effective in promoting immune responses in mice, type I IFN-inducing adjuvants have shown particular promise in nonhuman primate models (87, 88) and humans (89, 90) for promoting superior cellular and humoral immunity. The nanoparticle delivery strategy demonstrated here provides a simple means to promote both the safety and efficacy of CDNs as a novel type I IFN-promoting adjuvant, with potential relevance to human vaccine development. Altogether, these results suggest that LN-targeted CDNs can promote both strong antigen-specific T cell priming and high-titer, durable antibody responses that outperform the strong benchmark adjuvant MPLA, suggesting these compounds are of interest for further development as candidate adjuvants.

## Methods

**Materials.** Lipids 1,2-dioleoyl-*sn*-glycero-3-phosphocholine (DOPC), 1,2-dioleoyl-*sn*-glycero-3-phospho-(1-*rac*-glycerol) (DOPG), 1,2-dimyristoyl-*sn*-glycero-3-phosphocholine (DMPC), 1,2-distearoyl-*sn*-glycero-3-phosphoethanolamine-N-[methoxy(polyethylene glycol)-2000] (DSPE-PEG), and 1,2-distearoyl-*sn*-glycero-3-phosphoethanolamine-N-[PDP(polyethylene glycol)-2000] (DSPE-PEG-PDP) were purchased from Avanti Polar Lipids. Solvents, BSA and MPLA (from *Salmonella enterica* serotype minnesota Re 595 catalog L6895),

were purchased from Sigma-Aldrich. cdGMP was purchased from Invivogen, and cdGMP<sub>DY547</sub> was purchased from BIOLOG Life Science Institute and dissolved in ddH<sub>2</sub>O. The CD4<sup>+</sup> T cell helper peptides OT-II (CKISQAVHAAHAEINEAGREV) and HIV30 (RRNIIGDIRQAHCNISRAKW) and the MPER peptide (ELDKWASLWNWFNITNWLWYIK) were synthesized at the Tufts University Core Facility. SIINFEKL peptide was purchased from GenScript. MPER was purchased with either an N-terminal biotin (for ELISAs) or a palmitoyl tail (for immunizations). For membrane-anchored DSPE-HIV30 and DSPE-OT-II conjugates, HIV30 or OT-II were linked to DSPE-PEG-PDP via the cysteine residue of each peptide by dissolving HIV30 or OT-II in DMF with 1.5 equivalents of DSPE-PEG-PDP and agitating at 25°C for 18 hours. The conjugates were then diluted in 10x deionized water, lyophilized into powder, and redissolved in deionized water. Peptide concentrations were determined by Direct Detect infrared spectroscopy analysis (EMD Millipore). OVA used in the intracellular cytokine staining and tumor immunotherapy immunizations was purchased from Worthington Biochemical Corporation. Cysteine-terminated gp100 EGP long (CAVGALEGPRNQDWLVGPRQL) (91) was conjugated to DSPE-PEG-2000-maleimide from Laysan Biotechnology and purified as previously described (46).

**NP-MPER and NP-cdGMP synthesis.** A 2:2:1 molar ratio of DMPC/DOPC/DOPG in chloroform with palm-MPER added at a 1:200 MPER/lipid mole ratio was dried under nitrogen followed by incubation under vacuum at 25°C for 18 hours. Liposomes incorporating MPLA, DSPE-HIV30, or DSPE-OT-II were prepared by including these components in the organic solution prior to drying lipid films. Lipids were hydrated with pH 7.4 PBS to a final concentration of 26.5 mM lipid and vortexed 30 seconds every 10 minutes for an hour. The resulting NP-MPER vesicles were passed through 6 freeze-thaw cycles between liquid nitrogen and a 37°C water bath followed by extrusion 21 times through 0.2-µm pore polycarbonate membranes (Whatman Inc.), respectively. For NP-cdGMP, a 38:38:19:5:0.95 molar ratio of DMPC/DOPC/DOPG/DSPE-PEG/cdGMP in chloroform was dried under nitrogen followed by incubation under vacuum at 25°C for 18 hours, and following drying, the resulting lipid/cdGMP films were resuspended to a final concentration of 240 µg cdGMP per ml PBS and then freeze/thawed and extruded to form 150 nm liposomes. Unencapsulated cdGMP was removed by centrifugation of the liposomes via Airfuge (Beckman Coulter), and quantification of cdGMP encapsulation efficiency was determined by UV absorption at 254 nm. To synthesize cdGMP<sub>DY547</sub> lipid nanoparticles, cdGMP<sub>DY547</sub> was used in lieu of cdGMP at the lipid dry-down step. To synthesize fluorescently labeled “mock” cdGMP lipid nanoparticles, a dried lipid film of DMPC/DOPC/DOPG/DSPE-PEG (at a 38:38:19:5:0.95 molar ratio) was rehydrated in 520 µg/ml OVA<sub>AF647</sub> (Invitrogen) in PBS (lipid concentration = 35.6 mM) and synthesized as before. Dynamic light scattering (using a Wyatt Dyna Pro Plate Reader II) was performed by the Swanson Biotechnology Center at the Koch Institute.

**Mice and immunizations.** BALB/c, C56BL/6 (B6), C57BL/6J-Tmem173gt/J (STING<sup>Gt/Gt</sup>), and CD90.1 OT-II B6 mice were purchased from The Jackson Laboratory. Experiments were conducted using female mice, 6–8 weeks of age. Groups of mice were immunized with 100 µl MPER liposomes in PBS (40 µg MPER peptide) s.c. at the tail base, 50 µl per side. Where indicated, 100 µl soluble or liposomal cdGMP in PBS (5 µg cdGMP unless otherwise noted) was administered immediately following NP-MPER injection, s.c. at the tail base, 50 µl per side.

Sera were collected via retro-orbital bleeding on a weekly basis for subsequent ELISA-based analyses. For TNF-α blockade experiments, mice received 0.5 mg anti-TNF-α antibody (clone XT3.11, Bio X Cell) or IgG1 isotype control antibody (clone HRPN, Bio X Cell) i.p. at 24 hours and 0.5 hours prior to immunization, as described previously (81). For IFNαR1 blockade experiments, mice received 1 mg anti-IFNαR1 antibody (clone MARI-5A3, Bio X cell) or IgG1 isotype control antibody (clone MOPC-21, Bio X Cell) i.p. 24 hours prior to immunization, as described previously (92). For pDC depletion experiments, mice received 0.5 mg anti-PDCA1 antibody (clone 120G8, Bio X Cell) or IgG1 isotype control antibody (clone HRPN, Bio X Cell) i.p. at 48 hours prior to immunization (93). For polyfunctional T cell studies, B6 mice were immunized on days 0 and 14 with 10 µg OVA with blank PBS, 10 µg soluble cdGMP, or 10 µg NP-cdGMP, and PBMCs were collected on day 21 for intracellular cytokine staining. For tumor immunotherapy studies, B6 mice were inoculated s.c. in the right flank with 2.5 × 10<sup>5</sup> B16.F10 melanoma cells or 1 × 10<sup>6</sup> EG.7-OVA cells on day 0. In the EG.7-OVA model, mice were subsequently immunized on days 6, 13, and 20 with 10 µg OVA and blank PBS, 10 µg soluble cdGMP, or 10 µg NP-cdGMP. In the B16.F10 model, mice were immunized on days 5, 12, and 19 with 10 µg amph-gp100 and blank PBS, 10 µg soluble cdGMP, or 10 µg NP-cdGMP. Tumor area was measured via calipers over time, and PBMCs were collected 6 days after the second immunization for tetramer staining.

**CDN characterization studies.** For in vitro CDN release from lipid nanoparticles studies, aliquots of cdGMP<sub>DY547</sub> liposomes in PBS containing 10% BSA (dose of 1 µg cdGMP<sub>DY547</sub>) were placed into 10,000 MWCO Slide-A-Lyzer MINI Dialysis units (Thermo Fisher), and each aliquot was incubated in reservoirs of 10% BSA in PBS at 37°C. The presence of cdGMP<sub>DY547</sub> in reservoirs over time was measured (3 samples per time point) via fluorescence (excitation 545/emission 584) using a Tecan Infinite M200 Pro absorbance/fluorescence plate reader. For in vivo studies of LN drainage of CDN, mice were injected s.c. with 100 µl PBS (50 µl on each side of the tail base) containing 2 µg cdGMP<sub>DY547</sub> either in soluble or nanoparticle form. For each mouse, inguinal and axillary LNs were subsequently collected (3 mice per time point), pooled together, massed, and incubated for 18 hours in 1:25 Liberase TM (Roche) in PBS. LNs were then sonicated for 30 seconds at 3 watts output power using a Misonix XL-2000 probe sonicator. Following addition of 10% trichloroacetic acid in methanol, samples were centrifuged at 18,000 rcf for 15 minutes. Detection of cdGMP<sub>DY547</sub> in supernatants was measured via fluorescence (excitation 545/emission 584) using a Tecan Infinite M200 Pro absorbance/fluorescence plate reader.

**OT-II T cell adoptive transfer and ex vivo restimulation studies.** For adoptive transfer studies, OT-II<sup>+</sup> CD4<sup>+</sup> T cells were isolated from CD90.1 OT-II B6 mouse splenocytes using an EasySep CD4 T Cell Isolation Kit (StemCell Technologies) and transferred to C57BL/6 recipients by i.v. retro-orbital injection at 1 × 10<sup>5</sup> cells per mouse. Twenty-four hours later, mice were immunized with NP-MPER vaccines containing the DSPE-OT-II helper peptide. Seven days after immunization, inguinal and axillary LNs were collected for subsequent analysis via flow cytometry. For ex vivo OT-II restimulation studies, B6 mice were immunized on days 1, 28, and 42 with OT-II-containing vaccines. On day 49, 3 × 10<sup>5</sup> splenocytes in single-cell suspensions were seeded onto 96-well plates with or without 5 µM OT-II peptide and incubated for 48 hours, and cytokine levels in supernatants were assessed using a Milliplex MAP Mouse Th17 Magnetic Bead Kit from EMD Millipore and the Bio-Plex 3D suspension array system from Bio-Rad.

**Antibodies and flow cytometry.** For analyses of APCs, inguinal and axillary LNs were subjected to enzymatic digestion (Collagenase/Dispase and DNase I, Roche) in order to obtain single-cell suspensions as previously described (94). For processing of PBMCs, blood was subjected to 2 cycles of ACK lysis buffer incubation and washing in PBS. For all other flow cytometric-based analyses of LNs, single-cell suspensions were obtained by passage of tissues through a 70- $\mu$ m filter (BD Biosciences). Cells were incubated for 15 minutes at 25°C with anti-CD16/32 and then for 30 minutes at 25°C with the following antibodies (all purchased from eBioscience unless otherwise specified): CD4, CD69, CD11c, B220, CD11b, Ly6G, NK1.1, CD8 $\alpha$ , PDCA1 (eBio927), CD86, and MHC-II for the activation of APCs; B220, CD138, CD3, GL-7, IgD, and PNA for germinal center staining; CD90.1, CXCR5, CD8 $\alpha$ , CD4, B220, and CD44 for OT-II<sup>+</sup> CD4<sup>+</sup> T cell staining; and PE-H-2K<sup>b</sup> OVA (SIINFEKL) or PE-H-2D<sup>b</sup> gp100 (EGS-RNQDWL) tetramers (MBL International Corporation), CD8-APC, and DAPI for antigen-specific CD8<sup>+</sup> T cell staining. For intracellular cytokine staining, PBMCs were incubated for 6 hours at 37°C with OT-II and SIINFEKL peptides at a concentration of 10  $\mu$ g/ml each. Two hours into incubation with peptide, Brefeldin A (eBioscience) was added. Cells were surface stained with CD8 and CD4, fixed with Cytofix/Cytoperm (BD Biosciences), and stained intracellularly with IFN- $\gamma$  and TNF- $\alpha$  antibodies. Flow cytometric analysis was carried out using a BD Canto or BD Fortessa (BD Biosciences), and analysis of cells was performed using FlowJo software (Tree Star Inc.).

**Quantitative PCR analysis.** LNs were isolated from immunized mice, snap frozen in liquid nitrogen, and stored at -80°C for future use. Frozen LNs were homogenized, and RNA was isolated using the RNeasy Pluse Universal Mini Kit (Qiagen) according to the manufacturer's protocol. Total RNA was extracted using the RNeasy Plus Universal Kit (Qiagen) and quantified using a NanoDrop spectrophotometer (Thermo Fisher). Multiplex primers were designed using the PrimeTime qPCR assay (Integrated DNA Technologies). Primer sequences are as follows: mouse *Ifnb1*, (forward) 5'-CGAGCAGAGATCTTCAGGAAC-3' and (reverse) 5'-TCACTACCAGTCCCAGAGTC-3'; mouse *Rsad2*, (forward) 5'-ACACAGCCAAGACATCCTTC-3' and (reverse) 5'-CAAGTATTCACCCCTGTCCTG-3'; and mouse *Gapdh*, (forward) 5'-CTTTGTCAAGCTCATTCCTGG-3' and (reverse) 5'-TCTTGCTCAGTGCCTTGC-3'. One-step cDNA synthesis and RT-PCR reactions were set up with 200 ng total RNA using the LightCycler 480 RNA Master Hydrolysis Probes Kit (Roche) according to manufacturer's instructions, and analysis was performed on a Roche LightCycler 480 II real-time system.

**Plate- and bead-based ELISAs.** MPER-specific antibody levels were detected by ELISA: 96-well Nunc Polysorp plates (ThermoFisher) were coated with 25  $\mu$ g/ml streptavidin (Jackson ImmunoResearch),

blocked with 1% w/v BSA in PBS (BSA-PBS), washed with 0.05% Tween 20 in PBS, incubated for 2 hours with 2  $\mu$ g/ml biotin-MPER in BSA-PBS, washed, and then incubated for 2 hours with serially diluted serum samples. Following another washing step, the plates were incubated for 90 minutes with HRP-conjugated goat anti-mouse IgG (Bio-Rad) in BSA-PBS, washed, and developed with TMB substrate, and absorbance at 450 nm was read on a Tecan Infinite M200 Pro plate reader. HIV30-specific antibody levels were detected via ELISA in a similar manner; plates were directly coated with 100  $\mu$ g/ml HIV30, blocked, washed, and incubated with serum and IgG-HRP, as described above. Titers were defined as the inverse serum dilution, giving an absorbance of 0.3. To determine serum cytokine responses after immunization, sera were collected at 6 hours after immunization. Levels of IFN- $\beta$  were detected by the VeriKine-HS Mouse IFN- $\beta$  Serum ELISA Kit (PBL Assay Science), and levels of IFN- $\gamma$ , TNF- $\alpha$ , and IL-6 were determined by the Milliplex MAP Mouse Th17 Magnetic Bead Kit (EMD Millipore).

**Statistics.** Statistical analyses were performed using GraphPad Prism software. All values and error bars are mean  $\pm$  SD except where indicated differently. Comparisons of formulations over time used 2-way ANOVA tests, and comparisons of multiple formulations at a single time point were performed using 1-way ANOVA and Tukey's tests. Two-tailed unpaired *t* tests were used to determine statistical significance between two experimental groups for all other data, unless otherwise noted.

**Study approval.** Experiments and handling of mice were conducted under federal, state, and local guidelines under an IACUC protocol and with approval from the Massachusetts Institute of Technology IACUC.

## Acknowledgments

We thank Thomas Dubensky for helpful discussions on the biology of CDNs. We thank the Koch Institute Swanson Biotechnology Center and David Kanne for technical support. This work was supported in part by the Bill & Melinda Gates Foundation; The Ragon Institute of MGH, MIT, and Harvard; the NIH (AI091693 and AI095109); and the Koch Institute (Support [core] Grant P30-CA 14051 from the National Cancer Institute). G.L. Szeto is supported by the NIH under Ruth L. Kirschstein National Research Service Award 1F32CA180586. D.J. Irvine is an investigator of the Howard Hughes Medical Institute. K.D. Moynihan is supported by graduate fellowships from the Hertz Foundation and the National Science Foundation.

Address correspondence to: Darrell J. Irvine, 500 Main St., 76-261, Cambridge, Massachusetts 02139, USA. Phone: 617.452.4174; E-mail: djirvine@mit.edu.

- Koff WC, et al. Accelerating next-generation vaccine development for global disease prevention. *Science*. 2013;340(6136):1232-910.
- Rappuoli R, Mandl CW, Black S, De Gregorio E. Vaccines for the twenty-first century society. *Nat Rev Immunol*. 2011;11(12):865-872.
- Coffman RL, Sher A, Seder RA. Vaccine adjuvants: putting innate immunity to work. *Immunity*. 2010;33(4):492-503.
- Reed SG, Orr MT, Fox CB. Key roles of adjuvants in modern vaccines. *Nat Med*. 2013;19(12):1597-1608.
- Garçon N, Van Mechelen M. Recent clinical experience with vaccines using MPL- and QS-21-containing adjuvant systems. *Expert Rev Vaccines*. 2011;10(4):471-486.
- Dubensky TW, Kanne DB, Leong ML. Rationale, progress and development of vaccines utilizing STING-activating cyclic dinucleotide adjuvants. *Ther Adv*. 2013;1(4):131-143.
- Römling U, Galperin MY, Gomelsky M. Cyclic di-GMP: the first 25 years of a universal bacterial second messenger. *Microbiol Mol Biol Rev*. 2013;77(1):1-52.
- Ablasser A, et al. cGAS produces a 2'-5'-linked cyclic dinucleotide second messenger that activates STING. *Nature*. 2013;498(7454):380-384.
- Wu J, et al. Cyclic GMP-AMP is an endogenous second messenger in innate immune signaling by cytosolic DNA. *Science*. 2013;339(6121):826-830.
- Sun L, Wu J, Du F, Chen X, Chen ZJ. Cyclic GMP-AMP synthase is a cytosolic DNA sensor that activates the type I interferon pathway. *Science*. 2013;339(6121):786-791.

11. Ishikawa H, Barber GN. STING is an endoplasmic reticulum adaptor that facilitates innate immune signalling. *Nature*. 2008;455(7213):674–678.
12. Woodward JJ, Iavarone AT, Portnoy DA. c-di-AMP secreted by intracellular *Listeria monocytogenes* activates a host type I interferon response. *Science*. 2010;328(5986):1703–1705.
13. Burdette DL, et al. STING is a direct innate immune sensor of cyclic di-GMP. *Nature*. 2011;478(7370):515–518.
14. Karaolis DK, et al. Bacterial c-di-GMP is an immunostimulatory molecule. *J Immunol*. 2007;178(4):2171–2181.
15. Ebensen T, Schulze K, Riese P, Morr M, Guzmán CA. The bacterial second messenger c-di-GMP exhibits promising activity as a mucosal adjuvant. *Clin Vaccine Immunol*. 2007;14(8):952–958.
16. Yan H, et al. 3',5'-Cyclic diguanylic acid elicits mucosal immunity against bacterial infection. *Biochem Biophys Res Commun*. 2009;387(3):581–584.
17. Libanova R, et al. The member of the cyclic dinucleotide family bis-(3', 5')-cyclic dimeric inosine monophosphate exerts potent activity as mucosal adjuvant. *Vaccine*. 2010;28(10):2249–2258.
18. Ebensen T, Schulze K, Riese P, Link C, Morr M, Guzmán CA. The bacterial second messenger cyclic diGMP exhibits potent adjuvant properties. *Vaccine*. 2007;25(8):1464–1469.
19. Madhun AS, et al. Intranasal c-di-GMP-adjuvanted plant-derived H5 influenza vaccine induces multifunctional Th1 CD4<sup>+</sup> cells and strong mucosal and systemic antibody responses in mice. *Vaccine*. 2011;29(31):4973–4982.
20. Bosch V, et al. HIV pseudovirus vaccine exposing Env “fusion intermediates”-response to immunisation in human CD4/CCR5-transgenic rats. *Vaccine*. 2009;27(16):2202–2212.
21. Hu DL, Narita K, Hyodo M, Hayakawa Y, Nakane A, Karaolis DK. c-di-GMP as a vaccine adjuvant enhances protection against systemic methicillin-resistant *Staphylococcus aureus* (MRSA) infection. *Vaccine*. 2009;27(35):4867–4873.
22. Gray PM, et al. Evidence for cyclic diguanylate as a vaccine adjuvant with novel immunostimulatory activities. *Cell Immunol*. 2012;278(1–2):113–119.
23. Harrison LI, Astry C, Kumar S, Yunis C. Pharmacokinetics of 852A, an imidazoquinoline Toll-like receptor 7-specific agonist, following intravenous, subcutaneous, and oral administrations in humans. *J Clin Pharmacol*. 2007;47(8):962–969.
24. Chen W, Kuolee R, Yan H. The potential of 3',5'-cyclic diguanylic acid (c-di-GMP) as an effective vaccine adjuvant. *Vaccine*. 2010;28(18):3080–3085.
25. Irvine DJ, Swartz MA, Szeto GL. Engineering synthetic vaccines using cues from natural immunity. *Nat Mater*. 2013;12(11):978–990.
26. Storni T, Kündig TM, Senti G, Johansen P. Immunity in response to particulate antigen-delivery systems. *Adv Drug Deliv Rev*. 2005;57(3):333–355.
27. Jewell CM, López SCB, Irvine DJ. In situ engineering of the lymph node microenvironment via intranodal injection of adjuvant-releasing polymer particles. *Proc Natl Acad Sci U S A*. 2011;108(38):15745–15750.
28. Demento SL, et al. Role of sustained antigen release from nanoparticle vaccines in shaping the T cell memory phenotype. *Biomaterials*. 2012;33(19):4957–4964.
29. Bershteyn A, et al. Robust IgG responses to nanograms of antigen using a biomimetic lipid-coated particle vaccine. *J Control Release*. 2012;157(3):354–365.
30. Moon JJ, Suh H, Li AV, Ockenhouse CF, Yadava A, Irvine DJ. Enhancing humoral responses to a malaria antigen with nanoparticle vaccines that expand Tfh cells and promote germinal center induction. *Proc Natl Acad Sci U S A*. 2012;109(4):1080–1085.
31. Diwan M, Elamanchili P, Cao M, Samuel J. Dose sparing of CpG oligodeoxynucleotide vaccine adjuvants by nanoparticle delivery. *Curr Drug Deliv*. 2004;1(4):405–412.
32. Kasturi SP, et al. Programming the magnitude and persistence of antibody responses with innate immunity. *Nature*. 2011;470(7335):543–547.
33. Pihlgren M, et al. TLR4- and TRIF-dependent stimulation of B lymphocytes by peptide liposomes enables T cell-independent isotype switch in mice. *Blood*. 2013;121(1):85–94.
34. Xie H, et al. CpG oligodeoxynucleotides adsorbed onto polylactide-co-glycolide microparticles improve the immunogenicity and protective activity of the licensed anthrax vaccine. *Infect Immun*. 2005;73(2):828–833.
35. Coler RN, et al. A synthetic adjuvant to enhance and expand immune responses to influenza vaccines. *PLoS One*. 2010;5(10):e13677.
36. Ilyinskii PO, et al. Adjuvant-carrying synthetic vaccine particles augment the immune response to encapsulated antigen and exhibit strong local immune activation without inducing systemic cytokine release. *Vaccine*. 2014;32(24):2882–2895.
37. RTS,S Clinical Trials Partnership. Efficacy and safety of the RTS,S/AS01 malaria vaccine during 18 months after vaccination: a phase 3 randomized, controlled trial in children and young infants at 11 African sites. *PLoS Med*. 2014;11(7):e1001685.
38. Behzad H, et al. GLA-SE, a synthetic toll-like receptor 4 agonist, enhances T-cell responses to influenza vaccine in older adults. *J Infect Dis*. 2012;205(3):466–473.
39. Rose S, Misharin A, Perlman H. A novel Ly6C/Ly6G-based strategy to analyze the mouse splenic myeloid compartment. *Cytom A*. 2012;81(4):343–350.
40. Blume G, Cevc G. Liposomes for the sustained drug release in vivo. *Biochim Biophys Acta*. 1990;1029(1):91–97.
41. Oussoren C, Storm G. Lymphatic uptake and biodistribution of liposomes after subcutaneous injection: III. Influence of surface modification with poly(ethyleneglycol). *Pharm Res*. 1997;14(10):1479–1484.
42. Cai S, Yang Q, Bagby TR, Forrest ML. Lymphatic drug delivery using engineered liposomes and solid lipid nanoparticles. *Adv Drug Deliv Rev*. 2011;63(10–11):901–908.
43. Miyabe H, Hyodo M, Nakamura T, Sato Y, Hayakawa Y, Harashima H. A new adjuvant delivery system “cyclic di-GMP/YSK05 liposome” for cancer immunotherapy. *J Control Release*. 2014;184:20–27.
44. Chandra D, et al. STING ligand c-di-GMP improves cancer vaccination against metastatic breast cancer. *Cancer Immunol Res*. 2014;2(9):901–910.
45. Le Bon A, et al. Cutting edge: enhancement of antibody responses through direct stimulation of B and T cells by type I IFN. *J Immunol*. 2006;176(4):2074–2078.
46. Liu H, et al. Structure-based programming of lymph-node targeting in molecular vaccines. *Nature*. 2014;507(7493):519–522.
47. Gach JS, Leaman DP, Zwick MB. Targeting HIV-1 gp41 in close proximity to the membrane using antibody and other molecules. *Curr Top Med Chem*. 2011;11(24):2997–3021.
48. Montero M, van Houten NE, Wang X, Scott JK. The membrane-proximal external region of the human immunodeficiency virus type 1 envelope: dominant site of antibody neutralization and target for vaccine design. *Microbiol Mol Biol Rev*. 2008;72(1):54–84.
49. Dai G, Steede NK, Landry SJ. Allocation of helper T-cell epitope immunodominance according to three-dimensional structure in the human immunodeficiency virus type I envelope glycoprotein gp120. *J Biol Chem*. 2001;276(45):41913–41920.
50. Kim M, et al. Immunogenicity of membrane-bound HIV-1 gp41 membrane-proximal external region (MPER) segments is dominated by residue accessibility and modulated by stereochemistry. *J Biol Chem*. 2013;288(44):31888–31901.
51. Abdul-Sater AA, et al. The overlapping host responses to bacterial cyclic dinucleotides. *Microbes Infect*. 2012;14(2):188–197.
52. McWhirter SM, et al. A host type I interferon response is induced by cytosolic sensing of the bacterial second messenger cyclic-di-GMP. *J Exp Med*. 2009;206(9):1899–1911.
53. Crotty S. Follicular helper CD4 T cells (TFH). *Annu Rev Immunol*. 2011;29:621–663.
54. Sauer JD, et al. The N-ethyl-N-nitrosourea-induced Goldenticket mouse mutant reveals an essential function of Sting in the in vivo interferon response to *Listeria monocytogenes* and cyclic dinucleotides. *Infect Immun*. 2011;79(2):688–694.
55. Alving CR, Rao M. Lipid A and liposomes containing lipid A as antigens and adjuvants. *Vaccine*. 2008;26(24):3036–45.
56. Garaude J, Kent A, van Rooijen N, Blander JM. Simultaneous targeting of toll- and nod-like receptors induces effective tumor-specific immune responses. *Sci Transl Med*. 2012;4(120):120ra16.
57. Napolitani G, Rinaldi A, Bertoni F, Sallusto F, Lanzavecchia A. Selected Toll-like receptor agonist combinations synergistically trigger a T helper type 1-polarizing program in dendritic cells. *Nat Immunol*. 2005;6(8):769–776.
58. Cella M, et al. Plasmacytoid monocytes migrate to inflamed lymph nodes and produce large amounts of type I interferon. *Nat Med*. 1999;5(8):919–923.
59. Siegal FP, et al. The nature of the principal type 1 interferon-producing cells in human blood. *Science*. 1999;284(5421):1835–1837.
60. Swiecki M, Wang Y, Vermi W, Gilfillan S, Schreiber RD, Colonna M. Type I interferon negatively controls plasmacytoid dendritic cell numbers in vivo. *J Exp Med*. 2011;208(12):2367–2374.

61. Blaauboer SM, Gabrielle VD, Jin L. MPYS/STING-mediated TNF- $\alpha$ , not type I IFN, is essential for the mucosal adjuvant activity of (3'-5')-cyclic-di-guanosine-monophosphate in vivo. *J Immunol*. 2014;192(1):492-502.
62. Simon A, et al. Concerted action of wild-type and mutant TNF receptors enhances inflammation in TNF receptor 1-associated periodic fever syndrome. *Proc Natl Acad Sci U S A*. 2010;107(21):9801-9806.
63. Libanova R, Becker PD, Guzmán CA. Cyclic di-nucleotides: new era for small molecules as adjuvants. *Microb Biotechnol*. 2012;5(2):168-176.
64. Ouyang S, et al. Structural analysis of the STING adaptor protein reveals a hydrophobic dimer interface and mode of cyclic di-GMP binding. *Immunity*. 2012;36(6):1073-1086.
65. Shu C, Yi G, Watts T, Kao CC, Li P. Structure of STING bound to cyclic di-GMP reveals the mechanism of cyclic dinucleotide recognition by the immune system. *Nat Struct Mol Biol*. 2012;19(7):722-724.
66. Li XD, Wu J, Gao D, Wang H, Sun L, Chen ZJ. Pivotal roles of cGAS-cGAMP signaling in antiviral defense and immune adjuvant effects. *Science*. 2013;341(6152):1390-1394.
67. Ogunnanyi AD, et al. c-di-GMP is an effective immunomodulator and vaccine adjuvant against pneumococcal infection. *Vaccine*. 2008;26(36):4676-4685.
68. Ebensen T, Libanova R, Schulze K, Yevsa T, Morr M, Guzmán CA. Bis-(3',5')-cyclic dimeric adenosine monophosphate: strong Th1/Th2/Th17 promoting mucosal adjuvant. *Vaccine*. 2011;29(32):5210-5220.
69. McLennan DN, Porter CJ, Charman SA. Subcutaneous drug delivery and the role of the lymphatics. *Drug Discov Today Technol*. 2005;2(1):89-96.
70. Walder P, et al. Pharmacokinetic profile of the immunomodulating compound adamantylamide dipeptide (AdDP), a muramyl dipeptide derivative in mice. *Immunopharmacol Immunotoxicol*. 1991;13(1-2):101-119.
71. Kulkarni RR, et al. Activation of RIG-I pathway during influenza vaccination enhances germinal center reaction, promotes T follicular helper cell induction, and provides a dose-sparing effect and protective immunity. *J Virol*. 2014;88(24):13990-14001.
72. Smirnov D, Schmidt JJ, Capecchi JT, Wightman PD. Vaccine adjuvant activity of 3M-052: An imidazoquinoline designed for local activity without systemic cytokine induction. *Vaccine*. 2011;29(33):5434-5442.
73. Krupka M, et al. Enhancement of immune response towards non-lipidized *Borrelia burgdorferi* recombinant OspC antigen by binding onto the surface of metallochelating nanoliposomes with entrapped lipophilic derivatives of norAbu-MDP. *J Control Release*. 2012;160(2):374-381.
74. Wu CC, et al. Immunotherapeutic activity of a conjugate of a Toll-like receptor 7 ligand. *Proc Natl Acad Sci U S A*. 2007;104(10):3990-3995.
75. Wille-Reece U, et al. HIV Gag protein conjugated to a Toll-like receptor 7/8 agonist improves the magnitude and quality of Th1 and CD8<sup>+</sup> T cell responses in nonhuman primates. *Proc Natl Acad Sci U S A*. 2005;102(42):15190-15194.
76. Barker JR, et al. STING-dependent recognition of cyclic di-AMP mediates type I interferon responses during *Chlamydia trachomatis* infection. *MBio*. 2013;4(3):1-11.
77. Spörri R, Reis e Sousa C. Inflammatory mediators are insufficient for full dendritic cell activation and promote expansion of CD4<sup>+</sup> T cell populations lacking helper function. *Nat Immunol*. 2005;6(2):163-170.
78. Desch AN, et al. Dendritic cell subsets require cis-activation for cytotoxic CD8 T-cell induction. *Nat Commun*. 2014;5:4674.
79. Cucak H, Yrliid U, Reizis B, Kalinke U, Johansson-Lindbom B. Type I interferon signaling in dendritic cells stimulates the development of lymph-node-resident T follicular helper cells. *Immunity*. 2009;31(3):491-501.
80. Le Bon A, Schiavoni G, D'Agostino G, Gresser I, Belardelli F, Tough DF. Type I interferons potentially enhance humoral immunity and can promote isotype switching by stimulating dendritic cells in vivo. *Immunity*. 2001;14(4):461-470.
81. Parent MA, Wilhelm LB, Kummer LW, Szaba FM, Mullarky IK, Smiley ST. Gamma interferon, tumor necrosis factor alpha, and nitric oxide synthase 2, key elements of cellular immunity, perform critical protective functions during humoral defense against lethal pulmonary *Yersinia pestis* infection. *Infect Immun*. 2006;74(6):3381-3386.
82. Pasparakis M, Alexopoulou L, Episkopou V, Kollias G. Immune and inflammatory responses in TNF $\alpha$ -deficient mice: a critical requirement for TNF $\alpha$  in the formation of primary B cell follicles, follicular dendritic cell networks and germinal centers, and in the maturation of the humoral immune response. *J Exp Med*. 1996;184(4):1397-1411.
83. Waterhouse DN, Tardi PG, Mayer LD, Bally MB. A comparison of liposomal formulations of doxorubicin with drug administered in free form: changing toxicity profiles. *Drug Saf*. 2001;24(12):903-920.
84. Moon JJ, et al. Interbilayer-crosslinked multilamellar vesicles as synthetic vaccines for potent humoral and cellular immune responses. *Nat Mater*. 2011;10(3):243-251.
85. Friede M, Muller S, Briand JP, Van Regenmortel MHV, Schuber F. Induction of immune response against a short synthetic peptide antigen coupled to small neutral liposomes containing monophosphoryl lipid A. *Mol Immunol*. 1993;30(6):539-547.
86. de Titta A, et al. Nanoparticle conjugation of CpG enhances adjuvancy for cellular immunity and memory recall at low dose. *Proc Natl Acad Sci U S A*. 2013;110(49):19902-19907.
87. Tewari K, et al. Poly(I:C) is an effective adjuvant for antibody and multi-functional CD4<sup>+</sup> T cell responses to *Plasmodium falciparum* circumsporozoite protein (CSP) and  $\alpha$ DEC-CSP in non human primates. *Vaccine*. 2010;28(45):7256-7266.
88. Park H, et al. Polyinosinic-polycytidylic acid is the most effective TLR adjuvant for SIV Gag protein-induced T cell responses in nonhuman primates. *J Immunol*. 2013;190(8):4103-4115.
89. Caskey M, et al. Synthetic double-stranded RNA induces innate immune responses similar to a live viral vaccine in humans. *J Exp Med*. 2011;208(12):2357-2366.
90. Shirota H, Klinman DM. Recent progress concerning CpG DNA and its use as a vaccine adjuvant. *Expert Rev*. 2014;13(2):299-312.
91. van Stipdonk MJ, Badia-Martinez D, Sluiter M, Offringa R, van Hall T, Achour A. Design of agonistic altered peptides for the robust induction of CTL directed towards H-2Db in complex with the melanoma-associated epitope gp100. *Cancer Res*. 2009;69(19):7784-7792.
92. Teijaro JR, et al. Persistent LCMV infection is controlled by blockade of type I interferon signaling. *Science*. 2013;340(6129):207-211.
93. Asselin-Paturel C, Brizard G, Pin J-J, Brière F, Trinchieri G. Mouse strain differences in plasmacytoid dendritic cell frequency and function revealed by a novel monoclonal antibody. *J Immunol*. 2003;171(31):6466-6477.
94. Fletcher AL, et al. Reproducible isolation of lymph node stromal cells reveals site-dependent differences in fibroblastic reticular cells. *Front Immunol*. 2011;2:35.